IN-39
P-78

NASA Contractor Report 189078
RI/RD 91-219

Composite Load Spectra for Select Space Propulsion Structural Components

(Option I—Final Report)

James F. Newell and Hing W. Ho
Rockwell International
Canoga Park, California

December 1991

Prepared for
Lewis Research Center
Under Contract NAS3-24382

NASA
National Aeronautics and
Space Administration

Composite Load Spectra Option I Final Report

Table of Contents

Acknowledgement

The accomplishment of the Composite Load Spectra (CLS) project was a result of a Rocketdyne team working together and diligently on different aspects of the project. The authors would like to thank and acknowledge the contributions of our colleagues, Dr. D. Roy, Mr. R. J. Szabo, Mr. T. C. Hanshaw, Mr. S. Harvey and Mr. J. B. Gutierrez.

This work was sponsored by the NASA Lewis Research Center. The authors would like to thank Dr. C. C. Chamis, NASA program manager for the CLS program, for his vision and support of the CLS program, and Mr. D. Hopkins of NASA/LeRC for his support.

I. INTRODUCTION

The objective of this program is to develop generic load models, with multiple levels of progressive sophistication to simulate the composite (combined) load spectra that are induced in space propulsion system components, representative of Space Shuttle Main Engines (SSME), such as transfer ducts, turbine blades and liquid oxygen (LOX) posts (Ref. I.1). These models will be developed using two independent approaches. The first approach consists of developing a composite load spectra simulation methodology, using state-of-the-art probabilistic methods, to describe the individual loading conditions and combinations of these loading conditions and synthesize the composite load spectra.

The second approach, consists of developing coupled models for composite load spectra simulation which combine the (deterministic) models for composite load dynamic, acoustic, high-pressure and high rotational speed, etc., load simulation using statistically varying coefficients. These coefficients will then be determined using advanced probabilistic simulation methods with and without strategically selected experimental data. The first approach effort has been completed and work on the second approach started.

The unified theory required to combine the various individual load simulation models (hot-gas dynamic, vibrations, instantaneous-position, centrifugal field, etc.) into composite load spectra simulation models will be developed under this program. Results obtained from tests models will be compared with available numerical results with the loads induced by the individual load simulation models, and with available structural analysis results from independent analyses and tests. These theories developed under both approaches will be further validated with respect to level of sophistication and relative to predictive reliability and attendant level of confidence.

A computer code incorporating the various individual and composite load spectra models has been developed to construct the specific load model desired. The approach is to develop and deliver the computer code at intervals in the contract. The first version was an initial code for turbine blade loading. Subsequent code versions have added sophistication to the component probabilistic load definition and the decision making processes as well as installing a new set of loads for an additional component. This allows for ongoing evaluation and usage of the system by Rocketdyne and NASA.

II. SUMMARY OF PROGRESS DURING CLS OPTION I PERIOD

There are 4 significant accomplishments during the past year for CLS option I contract. They are: (1) the theoretical development works on the theory of the composite load spectra and the correlation field formalism; (2) the application of the CLS correlation field technology to the LOX post probabilistic structural analysis;

(3) the concentrated effort on development of a physical engine pressure fluctuation model and a vibration scaling model; and (4) the CLS load expert system LDEXPT version 3.0 with an extended influence coefficient set and a more structured and transportable code.

II.1 Composite Load Spectra Theory

The development of the Composite Load Spectra theory and its associated correlation field formalism has provided a firm theoretical foundation for the CLS technology which will facilitate future development and implementation of the technology (Ref. II.1). The correlation field formalism is a coupled model binding the engine system model and component models together and keeping track of correlation between system dependent loads and component loads. It provides a systematic approach to the composite load spectra synthesis. It solves the difficult correlation problem between the component loads in an elegant and yet intuitive way. The alternative is decomposing the random field into eigen states which may or may not correlate to the physical variables.

The CLS correlation field is especially suitable for use in perturbative probabilistic structural analysis. Each perturbation of the correlation field can be defined as a perturbation vector. The dot product of the perturbation vector and the correlation field (a vector field) will give the perturbed field to be supplied to the probabilistic structural analysis. The correlation of the component load thus generated to the engine hardware parameters and/or operation parameters is inherent in the correlation field. Therefore, the probabilistic structural analysis code does not need to be burdened with the detail of the space propulsion engine modeling and the interrelationship of engine parameters.

II.2 Application of the correlation field formalism

The application of the correlation field formalism to the LOX post probabilistic structural analysis was specially gratifying. In the study, the applicability of the CLS technology to the probabilistic structural analysis was demonstrated and the linkage procedure of the CLS program to the probabilistic structural analysis method (PSAM) program (Ref. II.2) was established. In the study, the stress responses and effective strain range of the LOX post as variation of the temperature and material property were evaluated by NESSUS developed for the PSAM program. Sensitivity factors of the effective strain range due to the independent random variables at different locations of the LOX post were obtained. This quantitative result provides valuable information for design and life evaluation of the LOX post.

II.3 Engine Pressure Fluctuation Model and Vibration Model

Under the Composite Load Spectra contract, a deterministic effort toward modeling fluid loading in engine/power systems was conducted from a Systems viewpoint. The goal was to identify noise sources and propagation effects in a complex engine/power system (Figure II.1); the process would lead to fluid-related failure prevention and better overall engine design. The four components, turbine blade, transfer duct, LOX post and HPOTP discharge duct selected as examples in the CLS effort all have had development problems in the SSME engine because of lack of knowledge, e.g. in modeling the flow energy in the system (acoustics waves defined as perturbed flow). Acoustic analysis methodologies employing physical models, using appropriate scaling criteria and considering uncertainties in their load values will enable probabilistic simulation to properly size hardware rather than fixing problems in the development program. The effort was directed toward the following subset of the total system effort.

(i) an acoustic propagation model, by which fluid acoustic/vibratory power could be transmitted to a critical structural part (example: pump sinusoidal power from a fuel pump to an engine duct).

(ii) a turned flow noise generation analysis, applicable for bends, T-sections, or similar parts of engine components such as the transfer duct. Technical efforts were focussed on finding a generalized model for any bend; some extensions and applications to other components have been made.

(iii) from numerous vibration data obtained in the past on various engine components, determine how it relates to acoustic fluid power for that component. This was pursued under a scaling technique, and the results show generic methods for a broad range of pumps and combustors. This method identifies "self-noise or vibration", which is a primary effect. There are also secondary coupling effects, such as vibration transmissions through structures and fluid ducts. Quantification of secondary effects will be pursued in the future.

Additional component noise source models development efforts separate from the CLS effort have been initiated to continue the overall flow system modeling development. These sources include pumps, combustors, and nozzles, etc. Two approaches to component noise modeling are in progress:

(a) Modeling important noise source mechanisms in pumps, and following the effect to the discharge duct.

(b) A non-generic effort, particularized to the SSME High Pressure Fuel Pump has been quantified. This work can provide a foundation for a generic model in the future.

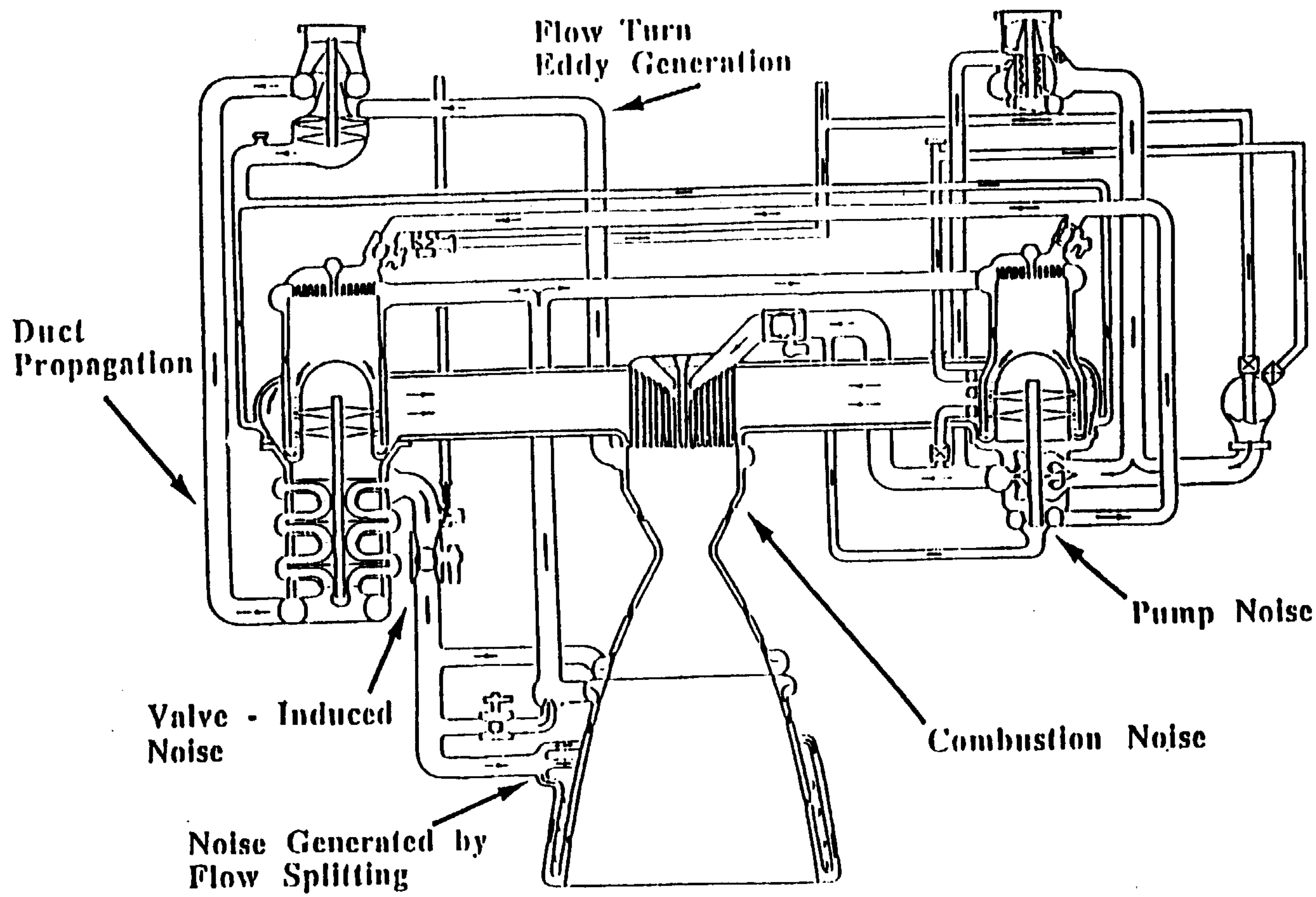

Figure II.1. SSME Noise Sources and Propagation

Coding of the pressure fluctuation propagation model (stand-alone PC version) was complete. It is a physical model describing the phenomenon of propagation of the pressure fluctuation. This is an advancement over the pedagogical model implemented in the base program.

II.4 CLS Load Expert System LDEXPT version 3.0

The expanded influence coefficient set (Ref. II.3) was implemented in the early phase of the CLS option I contract. The need for an expanded list of engine independent loads or parameters, dependent loads and thus influence coefficients was the result of the research effort during the CLS base program. It was found that the original influence model developed for engine performance analysis was inadequate in accounting for the engine-to-engine variations as caused by the variations in engine hardware parameters. The engine hardware variation was a result of variations in manufacture and in flight and test environments. The expanded list of engine system dependent loads was necessary also because of the requirement from additional component loads. The implementation of the expanded influence coefficient set was tested satisfactorily.

Improvements of the code planned has been complete. The Gaussian marginal distribution option for the correlation field was implemented. The HPFTP turbine blade finite element description was added to the load model for the turbine blade as an example model. New time step manager and mission phase manager routines were written. Uniform output to the "saved" file for the resultant distribution data for all loads was implemented. During the past year, numerous improvements were made to the code to improve its structure and modularity. The code was made more generic suitable for implementing additional loads for other components later on.

The CLS load expert system LDEXPT version 3.0 was implemented on the NASA/LeRC VM computing system. This version of LDEXPT has the expanded SSME engine influence coefficient set including 64 independent loads and 99 dependent loads. The lists of the independent and dependent load ID's, their default means and standard deviations are presented in Tables 1 and 2 of the CLS user's manual (see Appendix A). The influence coefficient set can be readily changed for any other engine. This was demonstrated as part of a separate study for the Advanced Launch Engine main combustion liner preliminary analysis.

The marginal distribution option is available in this version only for the Gaussian method. The marginal distributions are used to generate the correlation fields. This option is available to the example steady state turbine blade model (a full blade model for pressures and temperatures) and the full duty-cycle LOX post thermal model (transient start, steady state and transient cut-off).

Implementation of the Gaussian correlation field formalism using the marginal distribution was evolved as part of the LOX post study and were implemented as a part specific calculation. A generic procedure will be designed in the next phase of the contract effort and implemented so that the formalism will be applicable to any component.

A user manual for the CLS load expert system and an ANLOAD input file user's guide are presented in APPENDIX A.

III. THE CLS COUPLED MODEL AND THE CORRELATION FIELD FORMALISM

The Composite Load Spectra engine model has evolved into a multi-level coupled model as the development of component load models and their applications progresses. The physical coupling of the engine parts is simulated by the coupling between different levels of the CLS engine model through the interface loads. An abstract schematic of the multi-level engine model is shown in Figure III.1. It consists of an engine system model at the base of the multi-level model, subsystem loading environment models and component load models at the higher levels. The engine system model simulates the engine system to provide an engine environment for the subsystems to operate on. For an component within a complex subsystem, subsystem loading environment model is devised to correlate the engine system loads to the environment loading (or boundary loads) of the component. For example, the CLS LOX post thermal (temperature) model is a component load model using simple scaling based on the boundary loads: the maximum wall temperature on the hot gas side and the minimum wall temperature on the LOX (coolant) side. A thermal (boundary) load environment model was developed using the influence equation technique that correlates the system performance variables (e.g. hot gas flowrate and temperature, and LOX flowrate and temperature) to the boundary loads. This LOX post thermal environment model in turn couples with the engine system model so that the influence of the engine inlet conditions and hardware characteristics to the LOX post thermal load can be quantified. It is obvious that a proper accounting of the coupling or correlation of different levels of loads and variables is necessary to obtain a good estimate of the component loads. The CLS correlation field formalism was developed for just this purpose.

III.1 The Composite Load Spectra Correlation Field Formalism

The correlation field formalism presents a systematic approach to composite load spectra synthesis. The correlation field would have orthogonal components if the influences of appropriate independent loads are chosen as its components. Although orthogonality is not necessary it is a highly desirable property.

The composite load spectra for a space propulsion system component is a set of correlation fields. The correlation fields are func

Figure III.1

Composite Load Spectra

Multilevel Engine Model

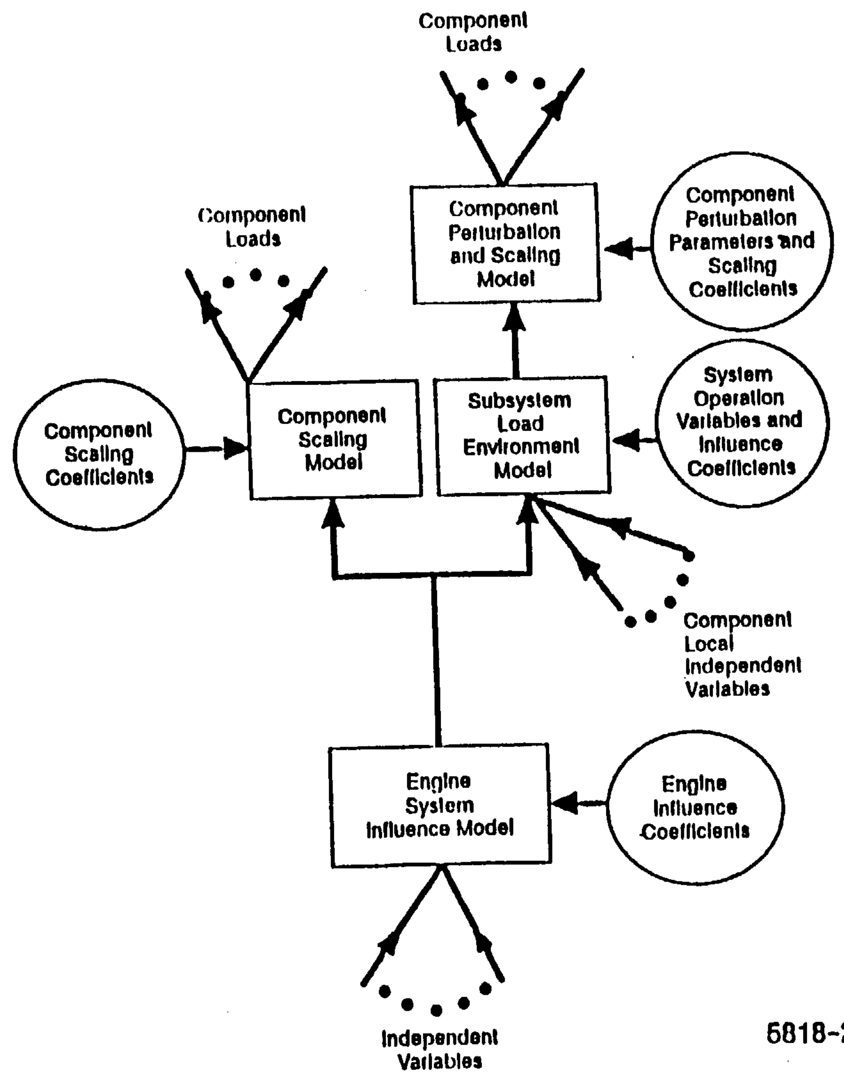

5818-2

tions of location (space coordinates) and time. Each correlation field represents a load distribution of the space propulsion system component.

Definition: **Composite Load Spectra** { CLSpectra } is defined as

$$\{ \mathit{CLSpectra} \} = \{ \Phi^{\alpha}(\vec{x}, t), \Phi^{\beta}(\vec{x}, t), \ldots \}$$

where $\Phi^{j}(\vec{x}, t)$'s are the correlation fields which are random vector fields defined in the probability space of the component loads $j = \alpha, \beta, \ldots$. This means that $\Phi^{j}(\vec{x}, t)$ have mean values and distributions defined on all locations $\vec{x}$ and all mission time t of the system components.

In CLS technology, the mean values of the component loads are obtained from measured data or from the calculated results of deterministic system models. These mean values are part of the knowledge base. The modeling effort of CLS, however, is centered on the evaluation of the component load random variations. In what follows, the random variation functions of the correlation fields are defined and the mean values of the correlation fields are implicitly assumed to be associated with the random variation functions and can be retrieved from the CLS load knowledge-based system.

Definition: **The correlation field** $\Phi^\alpha(\vec{x}, t)$ for component load α is a vector field, whose components are the marginal variation functions, each of which represents the variation of the load as caused by the random variable represented by the vector field component.[1]

$$\Phi^\alpha(\vec{x},t) = \phi_1^\alpha(\vec{x},t)\,\hat{I}_1 + \phi_2^\alpha(\vec{x},t)\,\hat{I}_2 + \ldots + \phi_n^\alpha(\vec{x},t)\,\hat{I}_n$$

where $\phi_i^\alpha(\vec{x}, t)$'s are the marginal variation functions for the ith vector field component. Each vector field component represents a random variable which contributes to the variation of the system component load.

Definition: **The marginal variation function** $\phi_i^\alpha(\vec{x}, t)$ for the system component load α and the vector field component i is a random variable defined in the probability space of the ith random variable. Its distribution is one of the marginal distribution function of the system component load α . The marginal variation function represents the gain or the variation of the system component load α induced by the variation of the ith random variable while keeping all other random variables constant.

---

[1] It is confusing to have the word "component" to mean different things. In the text, the space propulsion system component (the hardware component) is always referred to as the system component. The components of the correlation field, i.e. the vector components of the field is always referred to as the vector field component.

Definition: **The marginal distribution function** $f_i^m(L_\alpha)$ for the system component load α and the vector field component i is the partial integral of the joint distribution function for the system component of all random variables which contribute to the variation of the system component load α. The integration of the joint distribution is over all random variables except the ith random variable represented by the ith vector field component. The marginal distribution function $f_i^m(L_\alpha)$ described here is a distribution function over the ith random variable. It is not a distribution over the space coordinates and time. However, the distribution function is also a function of space and time because it represents the marginal distribution of a system component load as caused by a random variable at different space and time.

Theorem 1: The autocorrelation coefficient of a marginal variation function at two locations $\vec{x}_1$ and $\vec{x}_2$ is either +1 or -1.

$$\rho_i^{\alpha\alpha}(\vec{x}_1,\vec{x}_2) = \frac{\phi_i^\alpha(\vec{x}_1,t)\,\phi_i^\alpha(\vec{x}_2,t)}{|\phi_i^\alpha(\vec{x}_1,t)|\;|\phi_i^\alpha(\vec{x}_2,t)|}$$

$$= +1 \text{ or } -1$$

To show that the theorem is true, we will use the influence model as an example. The marginal variation of a system component load α as induced by the ith independent random variable can be evaluated as follow:

$$\Delta L_\alpha(\vec{x}_1) = b_1 \,\Delta L_i$$

$$\Delta L_\alpha(\vec{x}_2) = b_2 \,\Delta L_i$$

The difference in the influence coefficients is a result of the difference in scaling at the two locations. The autocorrelation is

$$R_{\alpha\alpha}{}^{i}(\vec{x}_1,\vec{x}_2) = COV(L_\alpha(\vec{x}_1),L_\alpha(\vec{x}_2))$$
$$= b_1 b_2 VAR(L_i)$$

and therefore the autocorrelation coefficient is

$$\rho_i{}^{\alpha\alpha} = \frac{R^i{}_{\alpha\alpha}(\vec{x}_1,\vec{x}_2)}{\sqrt{VAR(L_\alpha(\vec{x}_1))\,VAR(L_\alpha(\vec{x}_2))}}$$
$$= \frac{b_1 b_2 VAR(L_i)}{|b_1|\sqrt{VAR(L_i)}\,|b_2|\sqrt{VAR(L_i)}}$$
$$= +1 \; or \; -1$$

So theorem 1 is true at least for the influence model employed in CLS.

Definition: **The magnitude square of a random field** is defined as the variance of the random field.

$$|\Phi^{\alpha}(\vec{x},t)|^2 = VAR(\Phi^{\alpha}(\vec{x},t)) = E[\,\Phi^{\alpha}(\vec{x},t)\cdot\Phi^{\alpha}(\vec{x},t)]$$

The correlation fields and the marginal variation functions are random fields.

Definition: **The magnitude of a random field** is the square root of the magnitude square of the random field.

$$|\Phi^{\alpha}(\vec{x},t)| = \sqrt{|\Phi^{\alpha}(\vec{x},t)|^2} = \sqrt{VAR(\Phi^{\alpha}(\vec{x},t))}$$

Theorem 2: The magnitude square of the correlation field of a system component load is equal to the square sum of the magnitudes of the field components if the random variables that induce the variation of the system component load are independent.

$$|\Phi^{\alpha}(\vec{x},t)|^2 = |\phi_1^{\alpha}(\vec{x},t)|^2 + |\phi_2^{\alpha}(\vec{x},t)|^2 + \ldots$$

The quantity $|\,\Phi^{\alpha}(\vec{x},t)\,|$ measures the variation of the system component load α as caused by the random variations of the independent random variables. Whereas the quantity $|\,\phi_i^{\alpha}(\vec{x},t)\,|$ measures the marginal variation of the system component load α as caused by the ith independent random variable.

Definition: The **autocorrelation of a correlation field** at two locations $\vec{x}_1$ and $\vec{x}_2$ is the covariance of the correlation fields at $\vec{x}_1$ and $\vec{x}_2$, i.e. the expectation value of the dot product of the correlation fields at $\vec{x}_1$ and $\vec{x}_2$.

$$
\begin{aligned}
R_{\alpha\alpha}(\vec{x}_1,\vec{x}_2) &= COV(\Phi^{\alpha}(\vec{x}_1,t),\Phi^{\alpha}(\vec{x}_2,t)) \\
&= E\left[\ \Phi^{\alpha}(\vec{x}_1,t)\cdot\Phi^{\alpha}(\vec{x}_2,t)\right]
\end{aligned}
$$

Definition: The **autocorrelation coefficient of a correlation field** at two locations $\vec{x}_1$ and $\vec{x}_2$ is the ratio of the autocorrelation to the product of the magnitudes of the correlation field at the two locations.

$$
\rho^{\alpha\alpha}(\vec{x}_1,\vec{x}_2) = \frac{R_{\alpha\alpha}(\vec{x}_1,\vec{x}_2)}{|\Phi^{\alpha}(\vec{x}_1,t)|\cdot|\Phi^{\alpha}(\vec{x}_2,t)|}
$$

Theorem 3: The autocorrelation coefficient of a correlation field at any two locations is either +1 or -1 if only one random variable or field component is varied while the rest of random variables or field components are kept constant. i.e. In this case, $\rho^{\alpha\alpha}(\vec{x}_1, \vec{x}_2)$ becomes $\rho_i^{\alpha\alpha}(\vec{x}_1, \vec{x}_2)$ and

$$
\begin{aligned}
\rho_i^{\alpha\alpha}(\vec{x}_1,\vec{x}_2) &= \frac{\phi_i^{\alpha}(\vec{x}_1,t)\,\phi_i^{\alpha}(\vec{x}_2,t)}{\sqrt{(\phi_i^{\alpha}(\vec{x}_1,t))^2}\sqrt{(\phi_i^{\alpha}(\vec{x}_2,t))^2}} \\
&= +1 \ or\ -1
\end{aligned}
$$

Definition: **The cross-correlation of two correlation fields** is the covariance of the two correlation fields, i.e. the expectation value of the dot product of the two correlation fields.

$$R_{\alpha\beta}(\vec{x}_1, \vec{x}_2) = COV(\Phi^{\alpha}(\vec{x}_1, t), \Phi^{\beta}(\vec{x}_2, t))$$
$$= E\left[\Phi^{\alpha}(\vec{x}_1, t) \cdot \Phi^{\beta}(\vec{x}_2, t)\right]$$

Definition: **The cross-correlation coefficient of two correlation fields** is the ratio of the cross-correlation to the product of the magnitudes of the two correlation fields.

$$\rho^{\alpha\beta}(\vec{x}_1, \vec{x}_2) = \frac{R_{\alpha\beta}(\vec{x}_1, \vec{x}_2)}{|\Phi^{\alpha}(\vec{x}_1, t)| \cdot |\Phi^{\beta}(\vec{x}_2, t)|}$$

Theorem 4: The cross-correlation coefficient of two correlation fields corresponding to any two loads of a system component is either +1 or -1 if only one of the common random variables or field component is varied while the rest of the random variables or field components are kept constant. i.e. In this case, $\rho^{\alpha\beta}(\vec{x}_1, \vec{x}_2)$ becomes $\rho_i^{\alpha\beta}(\vec{x}_1, \vec{x}_2)$ and

$$\rho_i^{\alpha\beta}(\vec{x}_1, \vec{x}_2) = \frac{\phi_i^{\alpha}(\vec{x}_1, t)\, \phi_i^{\beta}(\vec{x}_2, t)}{\sqrt{(\phi_i^{\alpha}(\vec{x}_1, t))^2}\sqrt{(\phi_i^{\beta}(\vec{x}_2, t))^2}}$$
$$= +1 \text{ or } -1$$

It should be emphasized that the correlation field properties exhibit in theorems (2)-(4) are the results of the orthogonality of the random variables or field components of the correlation fields. It is possible to have non-orthogonal field components for the correlation fields. The formalism for using these non-orthogonal correlation fields in a probabilistic analysis would be very difficult. These remarkable properties of the orthogonal correlation fields enable the formalism to synthesize loads suitable for probabilistic structural analysis.

Perturbation of a correlation field can be evaluated by assigning a perturbation vector indicating the perturbations of each field component. e.g.

$$\vec{p}(\vec{x},t) = p_1\hat{I}_1 + p_2\hat{I}_2 + \ldots$$

where p_i 's are the fractional change of the random variable for the ith field component. The variation of the component load α is then

$$\begin{aligned} \Delta^{\alpha}(\vec{x},t) &= p(\vec{x},t)\cdot\Phi^{\alpha}(\vec{x},t) \\ &= p_1\phi_1{}^{\alpha}(\vec{x},t) + p_2\phi_2{}^{\alpha}(\vec{x},t) + \ldots \end{aligned}$$

All members of the composite load spectra { CLSpectra } for the system component of interest vary consistently according to the perturbation vector. Therefore, the correlations between different component loads, i.e. the correlations between the correlation fields within the composite load spectra are strictly maintained.

IV. THE LOX POST THERMAL LOAD CORRELATION FIELD

The LOX post thermal (temperature) load correlation field was synthesized as a demonstration of the correlation field methodology. It was applied to a probabilistic structural analysis of the LOX post whose structure and geometry are shown in Figure IV.1. The probabilistic analysis focused primarily on the influence of variation in the temperature load on the structural response, the stresses and the strain range (Ref. IV.1). The temperature correlation field simulates the influence of variation of the correlated system random variables and thus facilitates the analysis of the uncertainties affecting the structural response as caused by these random variables.

In this study, a component thermal load model of the LOX post developed in-house was implemented in the CLS load simulation code (Ref. IV.2). The component load model is coupled with the engine system model. The simulation code keeps track of the correlation between the component load and the system variables. To simplify the calculation, it was assumed that (1) the correlated field components were normally distributed and (2) only the variations of system performance variables and local heat transfer parameters were investigated, and (3) these performance variables and the heat transfer parameters were assumed to be independent. The component thermal load model being implemented for the LOX post is fairly generic. Thermal load for other components could be easily evaluated with the model if similar boundary condition scaling is used. For example, this thermal load model can be used for ducts. However, it is not a universal model. Thermal load model with different type of boundary condition scaling will need to be implemented separately.

Based on the LOX post (component) thermal load influence model, the LOX post thermal load varies as a function of the following eight (8) random variables: the hot gas temperature, the hot gas flowrate, the coolant temperature, the coolant flowrate, the hot gas mixture ratio, the heat shield gap geometry factor, the hot gas geometry factor related to the hot gas film heat transfer, and the coolant geometry factor related to the coolant film heat transfer. In this load simulation, the eight random variables are assumed to be independent and normally distributed. Since all random variables are normally distributed, a good variation function to be used is the sigma variable, which is the signed standard deviation of the marginal distribution. "Signed" means keeping the sign of the standard deviation with it.

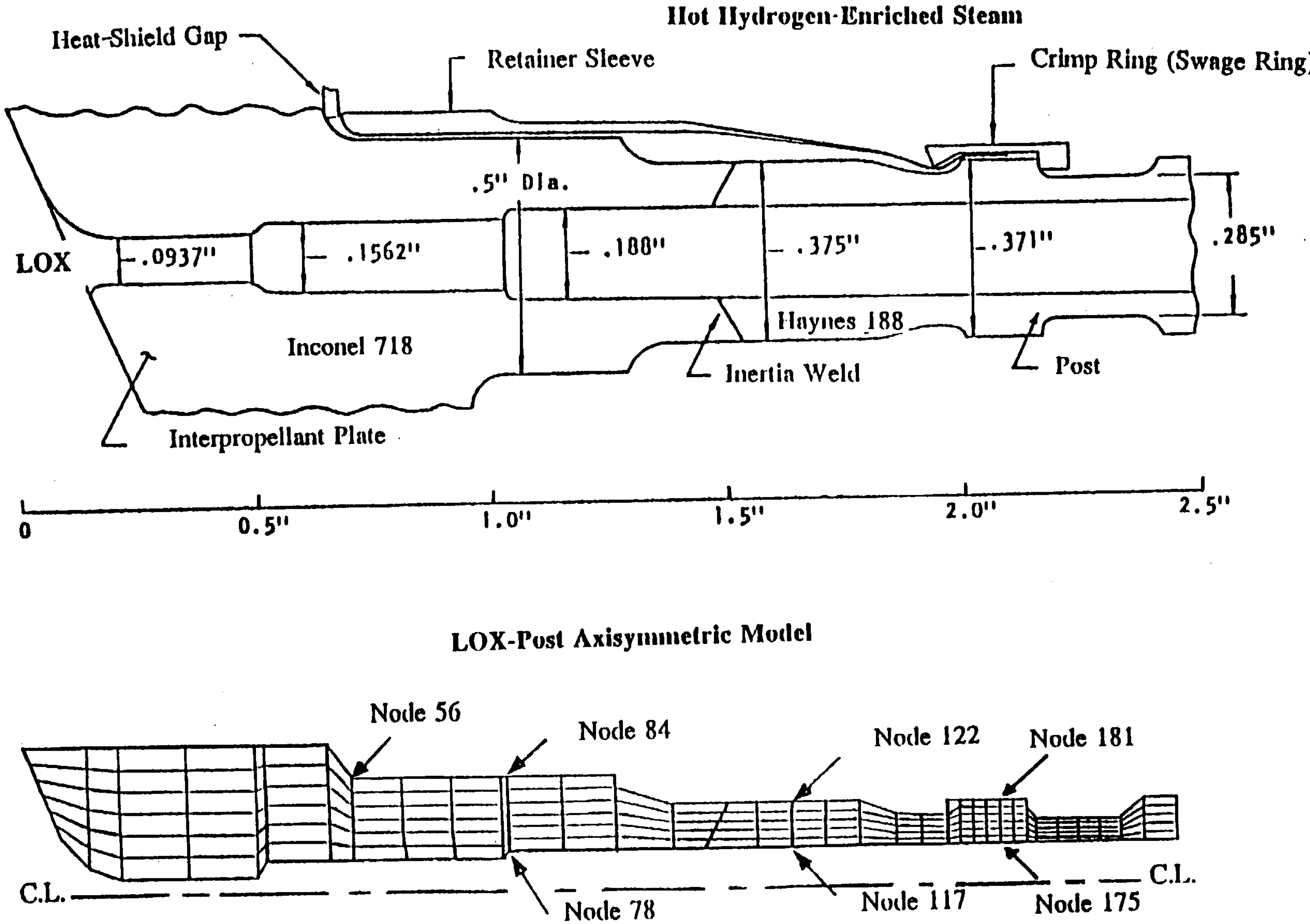

Figure IV.1. LOX Post and Its Axisymmetric Finite-Element Model

The LOX post thermal load correlation field is

$$
\begin{aligned}
\sigma^{T}_{LOXPost}(\vec{X}) = \; & \sigma^{HGT}(\vec{X})\,\hat{I}_{HGT} + \sigma^{HGF}(\vec{X})\,\hat{I}_{HGF} \\
& + \sigma^{CT}(\vec{X})\,\hat{I}_{CT} + \sigma^{CF}(\vec{X})\,\hat{I}_{CF} \\
& + \sigma^{MR}(\vec{X})\,\hat{I}_{MR} + \sigma^{GAP}(\vec{X})\,\hat{I}_{GAP} \\
& + \sigma^{HGG}(\vec{X})\,\hat{I}_{HGG} + \sigma^{CG}(\vec{X})\,\hat{I}_{CG}
\end{aligned} \tag{1}
$$

where, σ^{i} is the signed standard deviation of the marginal distribution of the LOX post temperature caused by the variation of the ith independent load. The sign of σ^{i} is defined as the sign of the variations to a +1 sigma variation of the ith independent load,

$\sigma^{HGT}(\vec{X})$ is the marginal distribution variation of the LOX post temperature as caused by the variation of the hot gas temperature,

$\sigma^{HGF}(\vec{X})$ is the variation as caused by hot gas flowrate,

$\sigma^{CT}(\vec{X})$ is the variation as caused by coolant temperature,

$\sigma^{CF}(\vec{X})$ is the variation as caused by coolant flowrate,

$\sigma^{MR}(\vec{X})$ is the variation as caused by mixture ratio,

$\sigma^{GAP}(\vec{X})$ is the variation as caused by heat shield gap geometry factor,

$\sigma^{HGG}(\vec{X})$ is the variation as caused by hot gas heat transfer film coefficient, and

$\sigma^{CG}(\vec{X})$ is the variation as caused by coolant heat transfer film coefficient.

The LOX post thermal load influence equation in a Gaussian moment form can be written as:

$$\sigma^{T}_{LOXPost}(\vec{X}) = (1-C_x)\,\sigma^{T}_{B1} + C_x\sigma^{T}_{B2} \tag{2}$$

$$\sigma^{T}_{B1} = b_{HGT,1}\sigma_{HGT}\hat{I}_{HGT} + b_{HGF,1}\sigma_{HGF}\hat{I}_{HGF} + \ldots \tag{3}$$

$$\sigma^{T}_{B2} = b_{HGT,2}\sigma_{HGT}\hat{I}_{HGT} + b_{HGF,2}\sigma_{HGF}\hat{I}_{HGF} + \ldots \tag{4}$$

where, σ^{T}_{B1} and σ^{T}_{B2} are the minimum and the maximum temperature boundary loads of the LOX post thermal load model used in the scaling equation (2),
the fractional temperature "distance"

$$C_x = \frac{T_x^{Ref} - T_{\min}^{Ref}}{T_{\max}^{Ref} - T_{\min}^{Ref}}$$

is the scaling constant at node $\vec{x}$,
T_{min}^{Ref} and T_{max}^{Ref} are the reference minimum and the reference maximum temperatures at the boundaries,
T_x^{Ref} is the reference temperature at node $\vec{x}$, the reference temperatures are the nominal values of the LOX post thermal load. The reference temperatures at all nodes are part of the database for the LOX post component load model,
σ_i 's are the standard deviations of the eight random variables,
$b_{i,j}$'s are the influence coefficients of the LOX post thermal load

model for the ith random variable and the jth boundary load. Substitute equations (3) and (4) into equation (2), and compare with equation (1), one obtains

$$\sigma^{i}(\vec{x}) = [(1-C_x)b_{i,1} + C_x b_{i,2}]\sigma_i \tag{5}$$

where, i ran through the set of indices { HGT, HGF, CT, CF, MR, GAP, HGG, CG }.

Express the variation functions in term of sensitivity factor form, the marginal variation function can be written as

$$\sigma^{T}{}_{LOXPost}(\vec{x}) = \sum_i \sigma^{i}(\vec{x})\,\hat{I}_i = \sum_i \frac{\partial\sigma^{T}}{\partial\sigma_i}\sigma_i \hat{I}_i \tag{6}$$

where ($\partial\sigma^{T}/\partial\sigma_{i}$) 's are the sensitivity factors.
From equations (5) and (6), the sensitivity factors are given as

$$\frac{\partial\sigma^{T}}{\partial\sigma_i} = (1-C_x)b_{i,1} + C_x b_{i,2} \tag{7}$$

The marginal sigma's (equation 2) are plotted in contoured plots. The mean temperatures of the LOX post is shown in Figure IV.2. A coupled of the sample marginal sigma's for the hot gas temperature and the heat shield gap factor are presented in Figures IV.3 and IV.4.

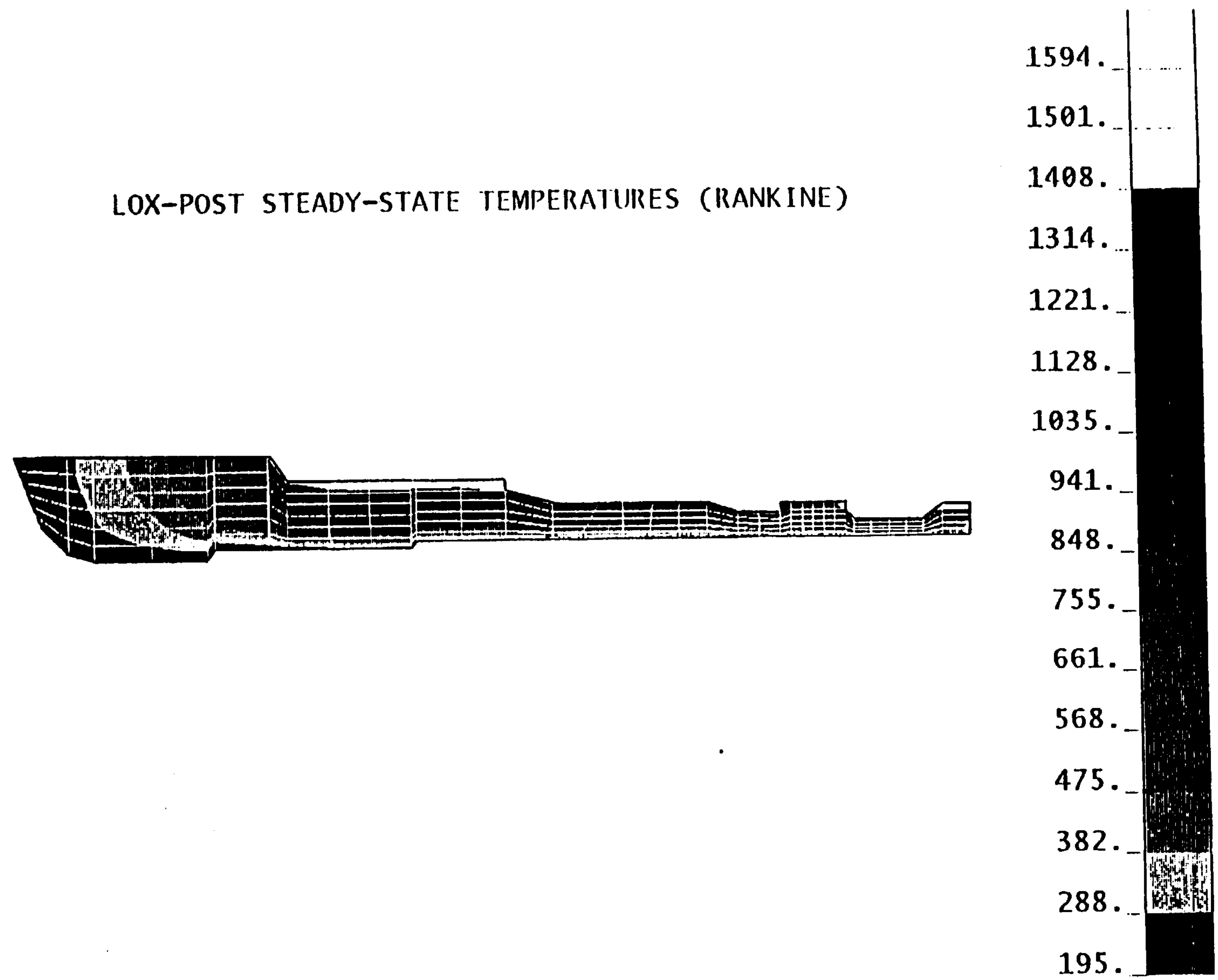

Figure IV.2. LOX Post Temperature Distribution at Steady State (Rankine)

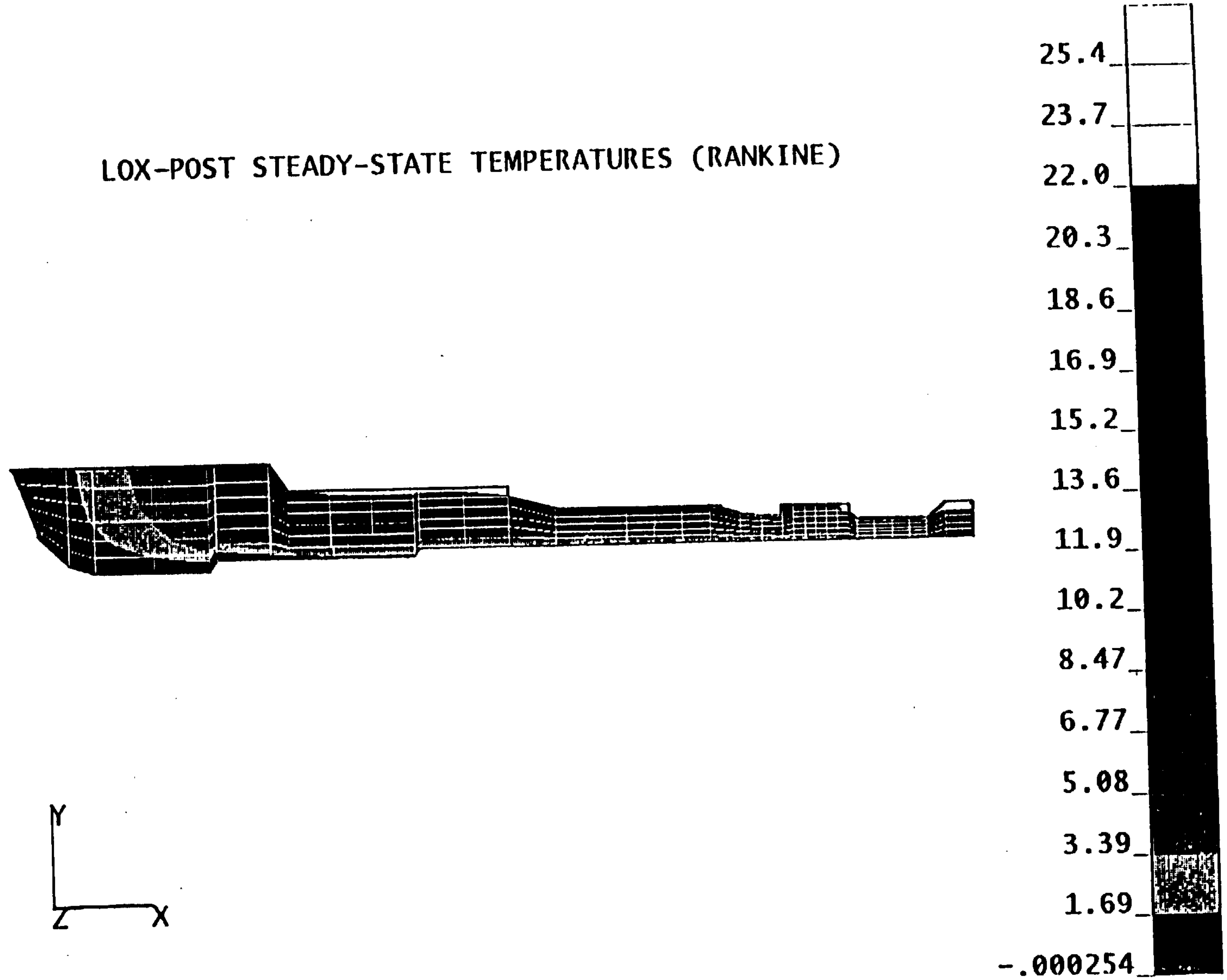

Figure IV.3. Correlation-Field Sensitivity Factors for the Hot-Gas Temperature Distribution on the LOX Post at Steady State

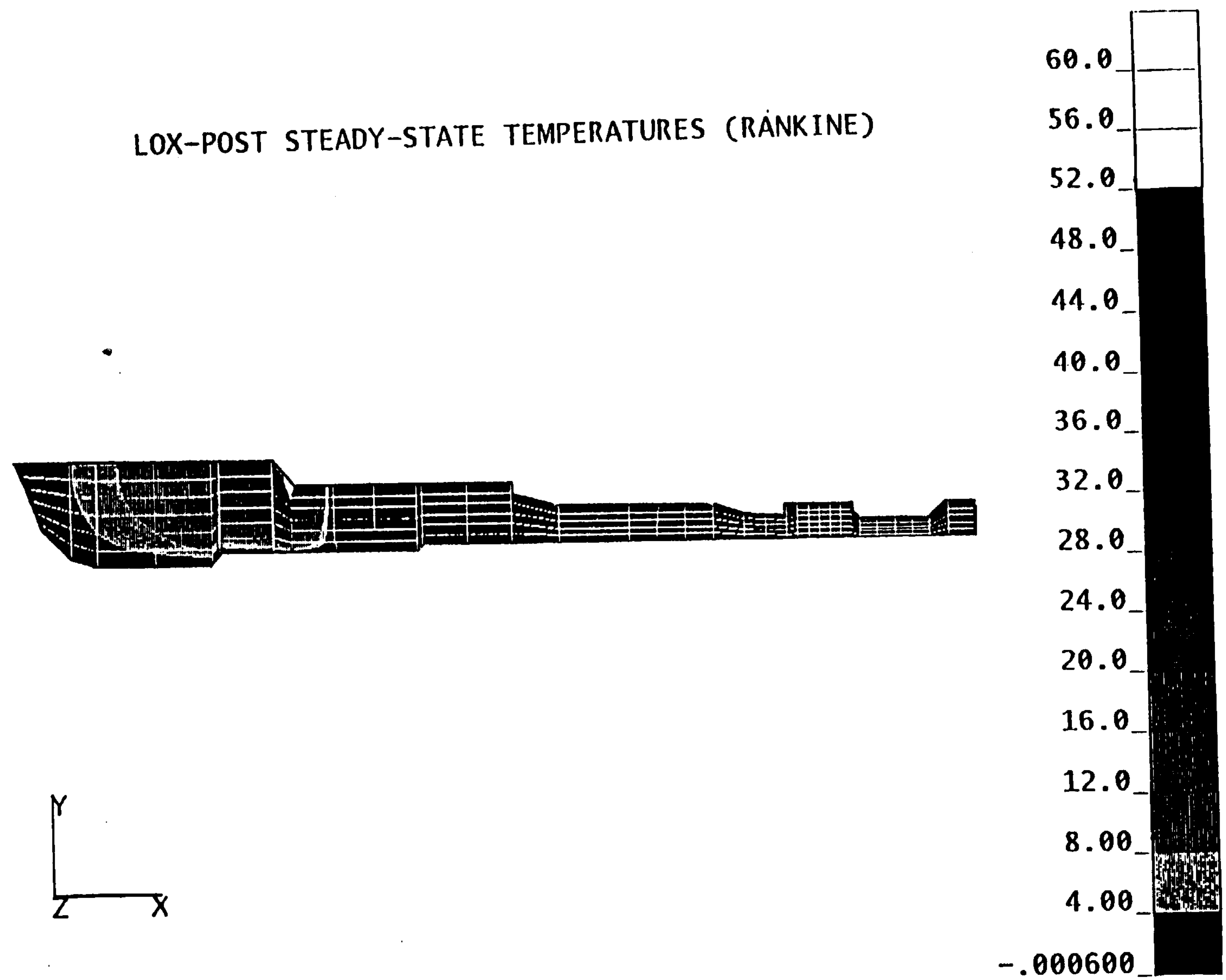

Figure IV.4. Correlation-Field Sensitivity Factors for the Heat-Shield-Gap Factor on the LOX Post at Steady State

The correlation fields for the LOX post temperatures during transient start and cutoff phases were also generated. In developing the LOX post thermal transient load model, a set of reference nodal temperature profiles of the LOX post at different times during the transient was employed to scale the mean temperatures and their variations. The advantage of this model is that the scaling is based on a realistic detailed thermal analysis result and gives an accurate simulation of the thermal transient load of the LOX post. The disadvantage of the model is that it is not as generic as one would like it to be because the model depends too much on the deterministic LOX post thermal analysis.

These transient loads together with the steady state load were used in a probabilistic structural analysis of the LOX post. Interested readers should consult the reference cited at the beginning of the this section.

V. COMPOSITE LOAD SPECTRA PHYSICAL MODELS

V.1 Engine Duct Pressure Fluctuation Model

Pressure fluctuations in a complex engine ducting system (e.g. the SSME) consists of four components (Ref. V.1). First, noise pressure fluctuations propagate from a noise source, for instance a pump. Second, there is noise generation at separation points in duct bends. Third, there is friction noise due to the attached flow in the duct. Fourth, the duct structural resonances could coincide with that of the pressure fluctuations in the fluid being carried in the duct. These four subjects are briefly discussed below.

(a) Noise Propagation : Currently, a one-dimensional noise pressure (acoustic) propagation model with multiple duct branching has been implemented in a computer code. Different ways of implementing duct losses have been considered and implemented. Considerable efforts have been given to identify a suitable actual SSME data set where the propagation effects dominate over the others for correlation against predicted results.

(b) Separated Flow Noise : A complete set of equations has been identified to model the separated flow noise sources. These fluctuations would be applied locally in the separated region and propagated by the propagation code described above. There is a rough scheme developed for future implementation of this method in a computer program.

(c) Attached Flow Friction Noise : For attached flow, an expression for the PSD has been obtained which is probably an improvement over other published literature (Ref. V.2). An expression has been developed which expresses both the real and imaginary parts of the cross - correlation fully. This approach enables a complete description of the fluctuation either in the time domain or in the frequency domain.

(d) Duct Resonance Effects : Duct resonance effects are either structural or acoustic related. These effects can be defined precisely. The acoustic resonance effect has been implemented in the propagation code. The structural resonance effect will be investigated for the next version of the code.

V.1.1 Fluid Acoustic Wave Propagation Algorithms

A general algorithm has been formulated to determine the pressure distribution as a function of time in a fluid ducting system which has been subjected to some unsteady loading. The method tracks acoustic waves generated by the loading, as they propagate through the fluid. The effects of those waves are used to determine the pressures and flowrates at any point in the system as a function of time. The algorithm is easy to implement and simple to understand from a physical standpoint. The method has been implemented as a

FORTRAN code FLAPR (Ref. V.3) both on the IBM/PC and the SUN workstations. Results can easily be converted from the time domain to the frequency response of the system. The method is applicable to a wide variety of problems.

The method has been tested with a number of textbook cases. In all cases the results match the expected results. The method has since been applied to a number of "real life" problems, with good results. Figure V.1(i) shows the application of FRAPR to the SSME low pressure fuel turbopump (LPFTP) discharge duct flex joint failure investigation. The result shows the gains between pressure at Elbow #1 and input pressure perturbation at LPFTP. Figure V.1(ii) shows the application of FRAPR as a muffler design tool.

V.2 **Pipe Bend Flow Noise (Turned Flow Noise)**

V.2.1 SUMMARY

A survey was conducted of the experimental literature on pressure fluctuations in straight and curved pipes. The test results quoted in various reports were used to obtain general predictive formulas for the local and propagated pressure spectra, correlation functions, and resultant force spectra for arbitrary bends in circular pipes. These formulas are recommended for use in determining the structural dynamic response of ducts to separated flow, turbulence, and propagated acoustic waves from duct elbows. These results are also applicable to turned flows in general, for example the flow into the transfer duct.

An extensive document was written in which these formulas were derived and explained and the phenomena they represent were discussed (Ref. V.4). The knowledge gained was applied to determine the resultant fluid force spectra in the bends of the low Pressure Fuel Pump Discharge Duct (Ref. V.5) under SSME funding. The formulas for the local and propagated pressure spectra were coded into a FORTRAN computer program called BENDS that resides on the SUN workstation. The BENDS code is linked to FLAPR that tracks acoustic waves from sources like pipe bends through a complex ducting system.

V.2.2 DEVELOPMENT

Two reports (Ref. V.6 and V.7) were found in which arrays of pressure transducers were used to measure the fluctuating pressure fields in two different 90 degree pipe elbows. This data was used to define the spatial distribution of the root mean square fluctuating pressure in a bend (Figure V.2). Although the elbows were both 90 degrees their curvatures were different. This provided information regarding the dependence of the pressure fluctuations on bend curvature.

Figure V.1. Noise Propagation and Acoustic Modes Analysis

Transfer function analysis: Gain and Phase

(i) Problem diagnosis

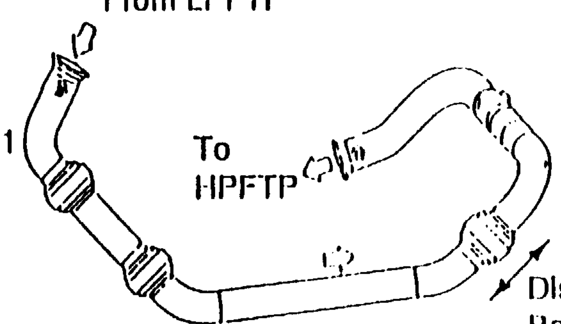

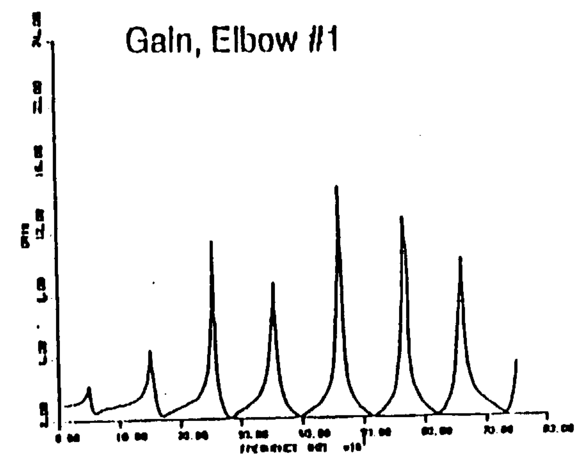

(ii) Design tool

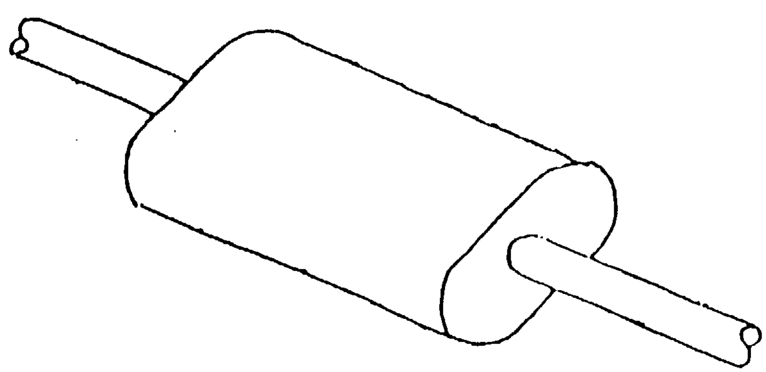

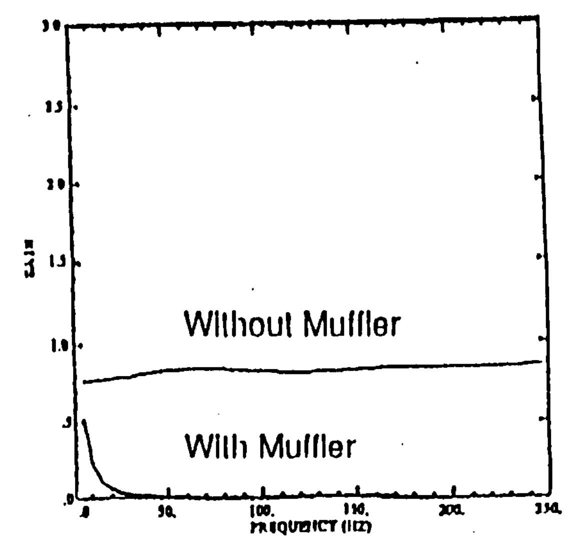

Rockwell International
Rocketdyne Division

90ALS-132-167

ORIGINAL PAGE IS
OF POOR QUALITY

ACTUAL RMS PRESSURE DISTRIBUTION

APPROXIMATION USING STEP FUNCTIONS AND EXPONENTIALS IN THIS REPORT

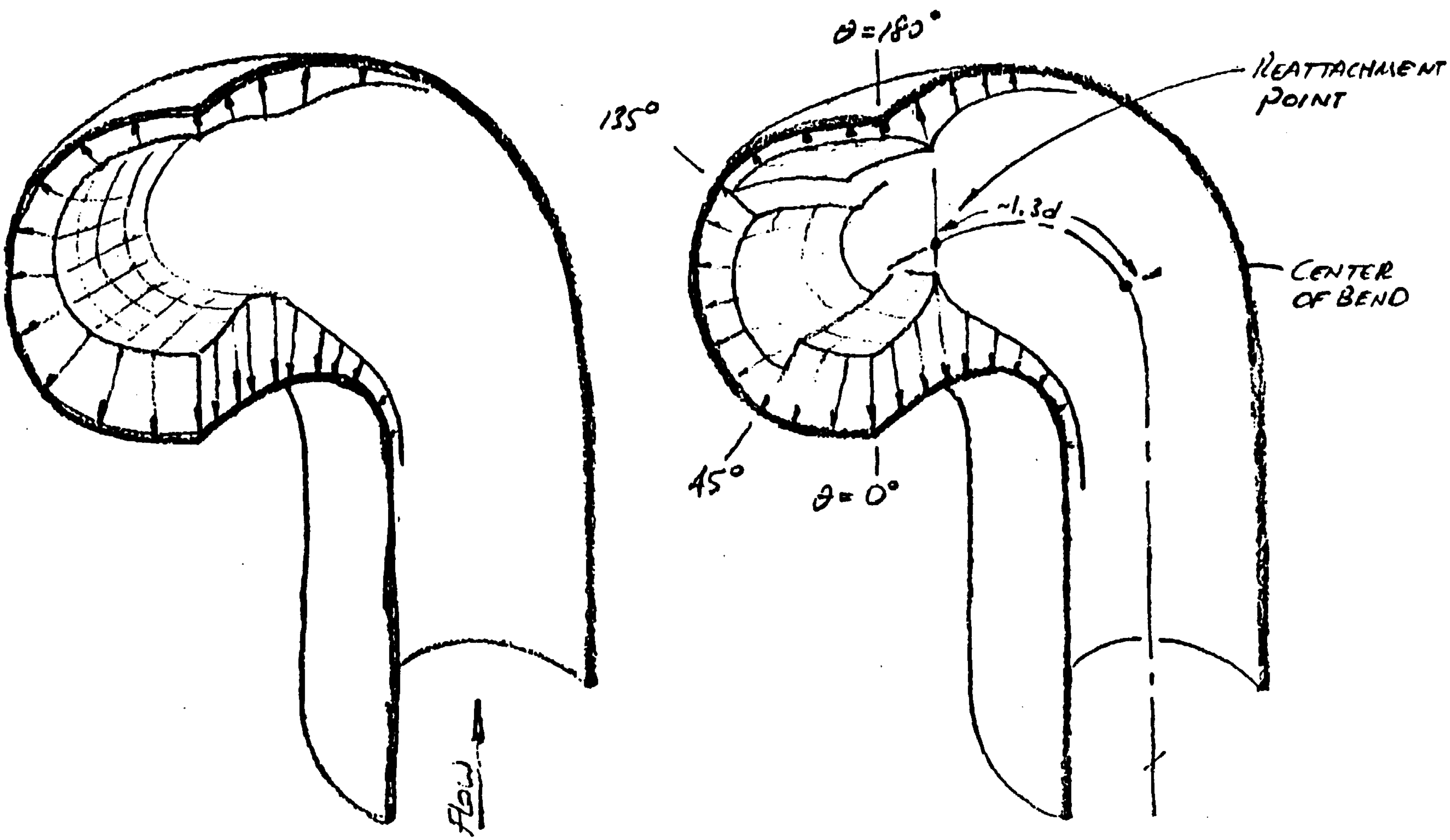

Figure V.2. SPATIAL DISTRIBUTION OF RMS PRESSURE IN A PIPE BEND

A paper (Ref. V.8) on the steady state pressure drop across elbows with different turning angles was used to infer the dependence of the local fluctuating pressures on turning angle. Direct measurements of the fluctuating pressure fields in other than 90 degree elbows was not found.

Fluctuating pressure spectra were obtained from References V.6 and V.7 for locations on the inside and outside walls of the bends and for locations upstream and downstream of where the flow separates and reattaches. It was found that the shapes of the spectra were independent of measurement location. The measurement location only effected the magnitude of the spectra.

Additional pressure spectra were obtained at isolated points in three other duct bends (Ref. V.9 and V.10). It was found that when the amplitudes of the pressure spectra were normalized by the composite root mean square fluctuating pressure and when frequency was nondimensionalized using the flow velocity and duct diameter the resulting nondimensionalized pressure spectra from References V.6, V.7, V.9, and V.10 fit fairly well on top of one another (Figure V.3). A prediction formula for the normalized pressure spectrum was drawn through the experimental normalized spectra. The peak, break point, and final slope in the prediction formula were interpreted respectively in terms of the maximum eddy size in the pipe, the separation bubble length, and the Kolmogorov turbulence spectrum.

Turbulent fluctuating pressure correlation measurements were not found for flows through bends but were available for flows through straight pipes (Ref. V.11) and over flat plates (Ref. V.12). These measurements suggest that the primary cause of turbulent wall pressure fluctuations is the convection of many different sizes of eddies over the wall. The convection velocity depends only weakly on eddy size. The convection velocity and the frequency dependence of eddy size was deduced from the straight pipe measurements of Reference V.11. It is assumed that these relations apply to curved pipes and elbows as well.

The correlation measurements, convection velocity, and eddy sizes from Reference V.11 were used to derive an expression for the cross spectral density of the fluctuating pressure field. The cross spectral density is a frequency dependent expression that combines information on the pressure spectra with information on spatial and temporal correlations. An expression relating the correlation length of the fluctuating pressure field to frequency was also derived. Higher frequency pressure fluctuations have smaller correlation lengths. The correlation length function is needed when performing flow induced vibration analyses of plate or shell structures.

The formulas for the spatial amplitude distribution and the cross spectral density of the fluctuating pressure field were used to derive expressions for resultant force spectra that the flow

Figure V.3. Generic Flow Turning Noise Spectral Shape

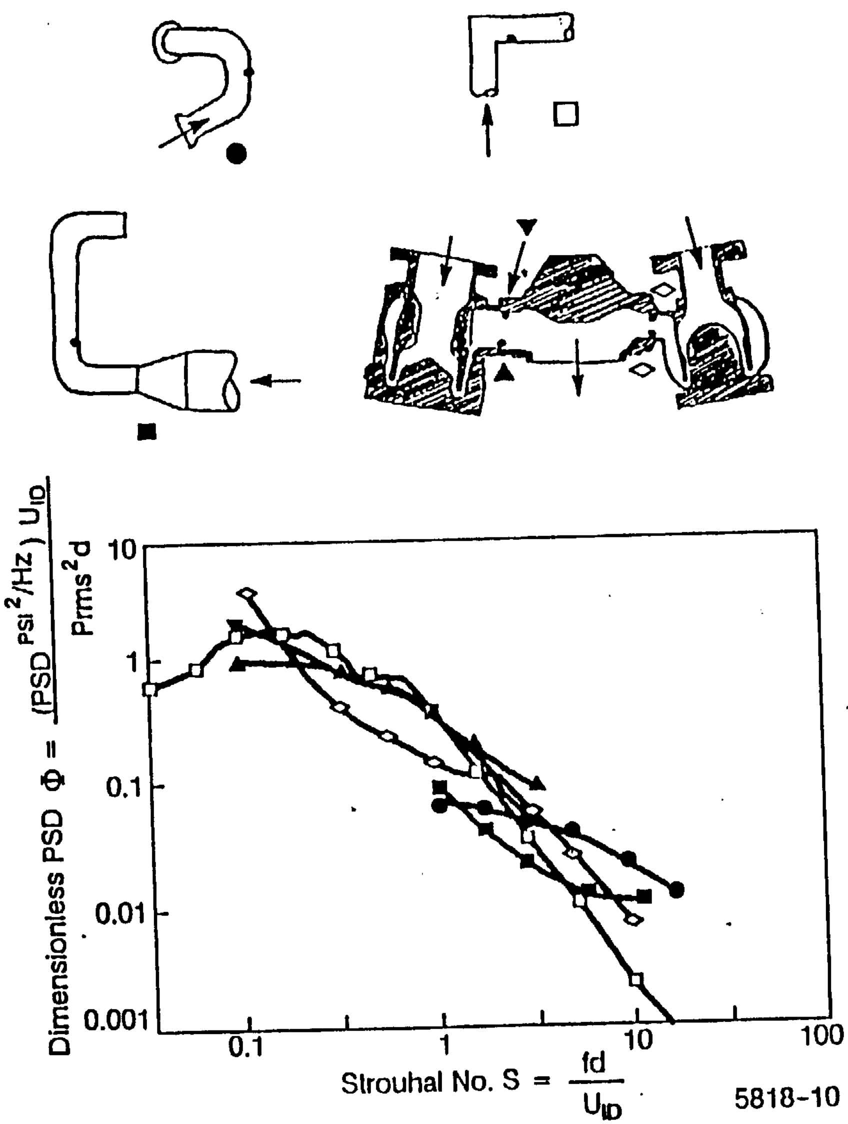

Dimensionless Power Spectral Density for Different Flows

applies to an arbitrary bend. One of the expressions is for the resultant force in the plane of the bend and the other is for the resultant force perpendicular to the plane of the bend. These expressions are extremely useful since they provide dynamic flow loading that are easy to calculate and easy to apply in a structural dynamic analysis. With these expressions the effects of a complicated turbulent pressure field are reduced to just two point force spectra that may be applied to a finite element duct modeled as a series of beams (Figure V.4).

Fluctuating pressures were measured very far downstream of the elbow in Reference V.6. The fluctuating pressure as a function of downstream location appeared to approach an asymptotic value that was significantly higher than the fluctuating pressure one would expect in a straight pipe without an elbow. Furthermore, step increases in the pressure spectra were observed where one would expect the first and second diametral duct modes to cut on. Therefore, the authors of Reference V.6 concluded that the pressure measured at the far downstream location was primarily due to acoustic propagation from the elbow. The ratio between the propagated acoustic pressure at the far downstream location and the peak local pressure in the elbow was calculated. Since no other report giving both of these measurements was found, it is assumed that this ratio between the propagated acoustic pressure and the peak local elbow pressure holds for all pipe bends.

Expressions for the propagated acoustic plane wave and first diametral pressure spectra were defined in terms of the peak local elbow pressure spectrum. Reference V.13 shows a significant increase in the sound radiated into the outside air from a pipe at frequencies above the first diametral cut on frequency. This suggests that the kinds of acoustic waves in a duct have a significant effect on the duct vibration. The possible effects of plane waves and first diametral waves on duct vibration were considered.

The formulas derived for the local and propagated pressure spectra in a pipe with an arbitrary elbow were coded into a FORTRAN program called BENDS. This program currently resides on the SUN workstation. The BENDS program is linked to another program called FLAPR that tracks acoustic waves emanating from sources such as pipe elbows through a complex ducting system.

As more experimental data becomes available it will be incorporated into the formulas developed in this project. In particular, more measurements of the pressure fields in different elbows are being sought. More measurements of both the local and propagated acoustic pressure in bends is necessary to strengthen the relationship between the two. The relationship between these and the mean pressure loss across an elbow should be explored. Measurements of correlation functions in elbows should be obtained. A test should be run in which the resultant flow force spectra on a bend are measured directly.

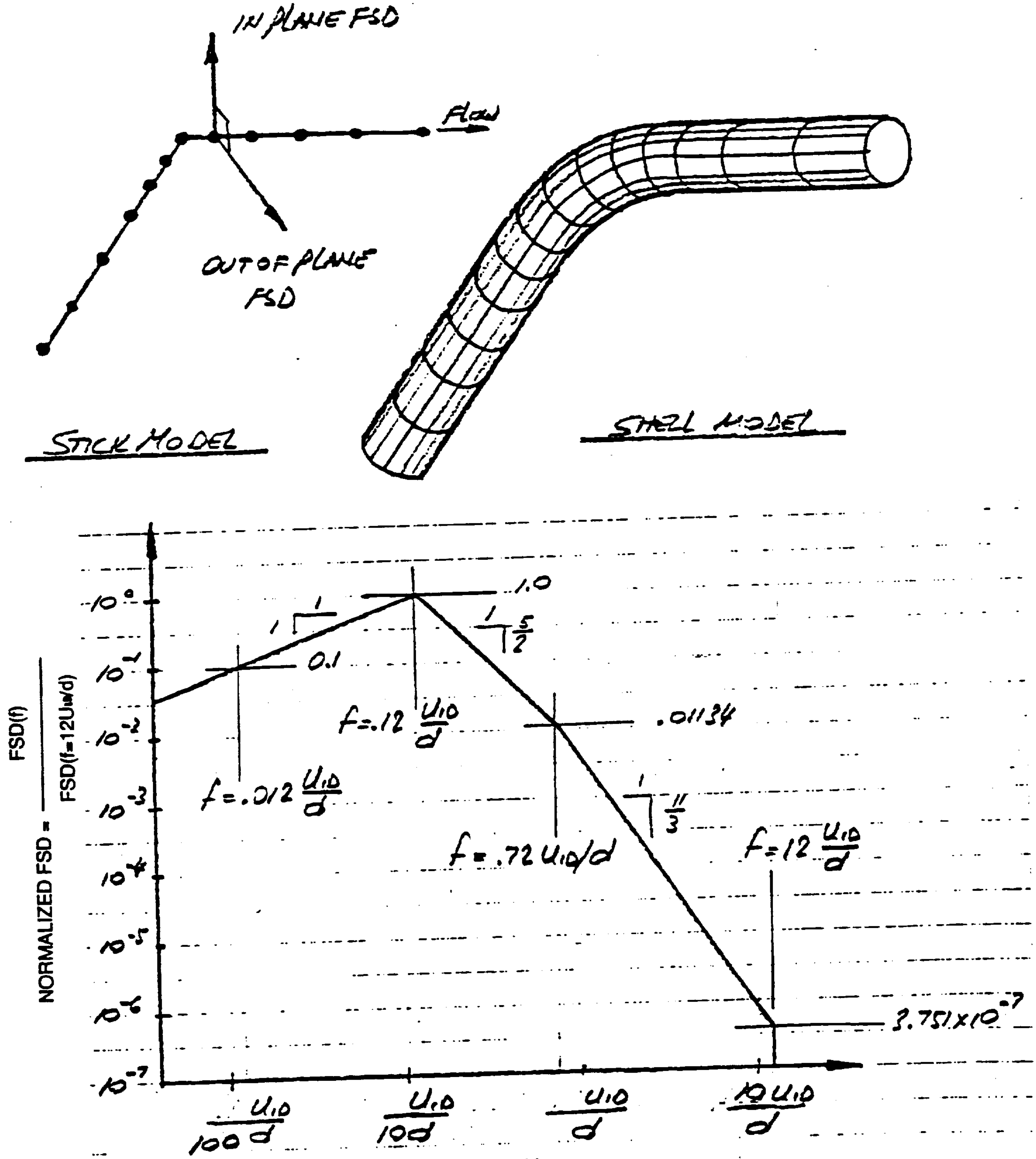

Figure V.4. NORMALIZED POWER SPECTRAL DENSITY OF THE RESULTANT FLUCTUATING FORCES IN A PIPE BEND

V.3 Component Scaling Criteria of Vibration

The vibrational environment is an important consideration in determining the loads on an engine. The composite load spectra component scaling criteria (CLS-CSC) is an enhanced method of estimating the vibrational loads on a component based on similitude with a reference component. A component based scaling has a distinct advantage over past global scaling methods since many engine components (such as pumps, turbines, preburners, combustors, etc.) generate a significant part of their own vibration. Therefore the local physics of the component can be used to estimate the vibrational environment. Component scaling methods enable simple means of estimating the vibrational environments of future rocket engine systems based on past designs.

The original scaling criteria put forth by R. E. Barrett (Ref. V.14) estimated the loads globally based on the total specific power of the rocket engine (thrust times exhaust velocity). The CLS-CSC estimates the vibrational load of components based on a component specific power. A specific power is determined for each component that reflects the rms level of the dominant forcing function. From this specific power the vibrational load of each component is estimated. The vibrational load on a component is determined by a similitude or scaling relation to a reference system. Like the Barrett Criteria, the CLS-CSC method does not consider any differences in rotordynamic or acoustic resonances between the reference and new components that might exist.

The intention of the CLS-CSC is to provide a tool, free of complex calculations, to estimate the broadband vibrational load on rocket engine components at different operating points and to estimate the vibrational load on a similar component (Ref. V.15). Currently estimates of the vibrational environment of turbopumps (Figure V.5) and combustion chambers, to a lesser extent, (Figure V.6) are possible using the CLS-CSC method.

V.3.1 TURBOPUMPS

The vibration scaling for turbopumps uses an enhanced scaling criterion. This citerion is summarized in the equation.

$$\left(\frac{G^2{}_{rms}}{Ps}\right)_{NEW} = \left(\frac{G^2{}_{rms}}{Ps}\right)_{REFERENCE}$$

Figure V.5. CLS Method Applied to SSME Turbopumps

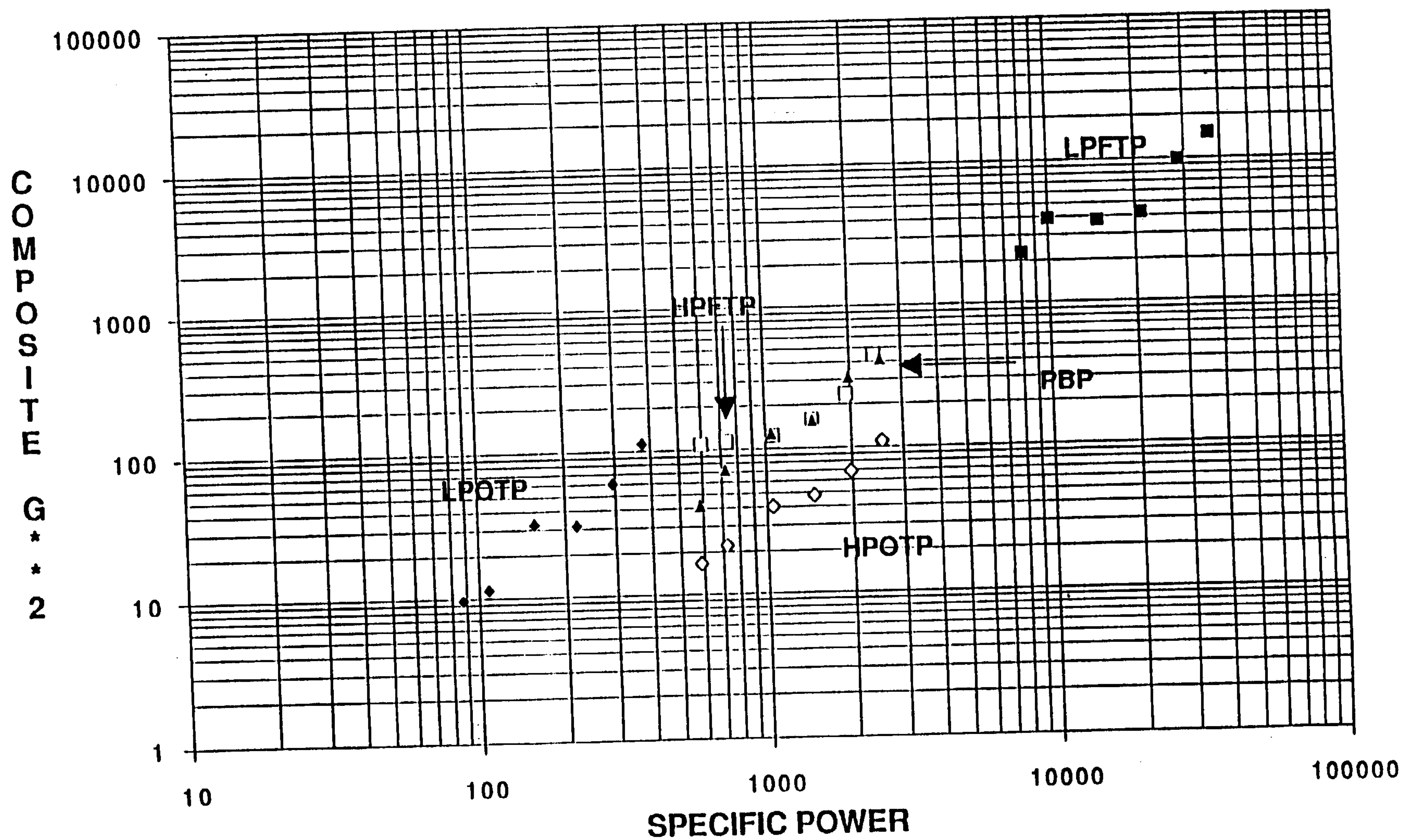

Figure V.6. CLS Combustion Chamber Scaling Method

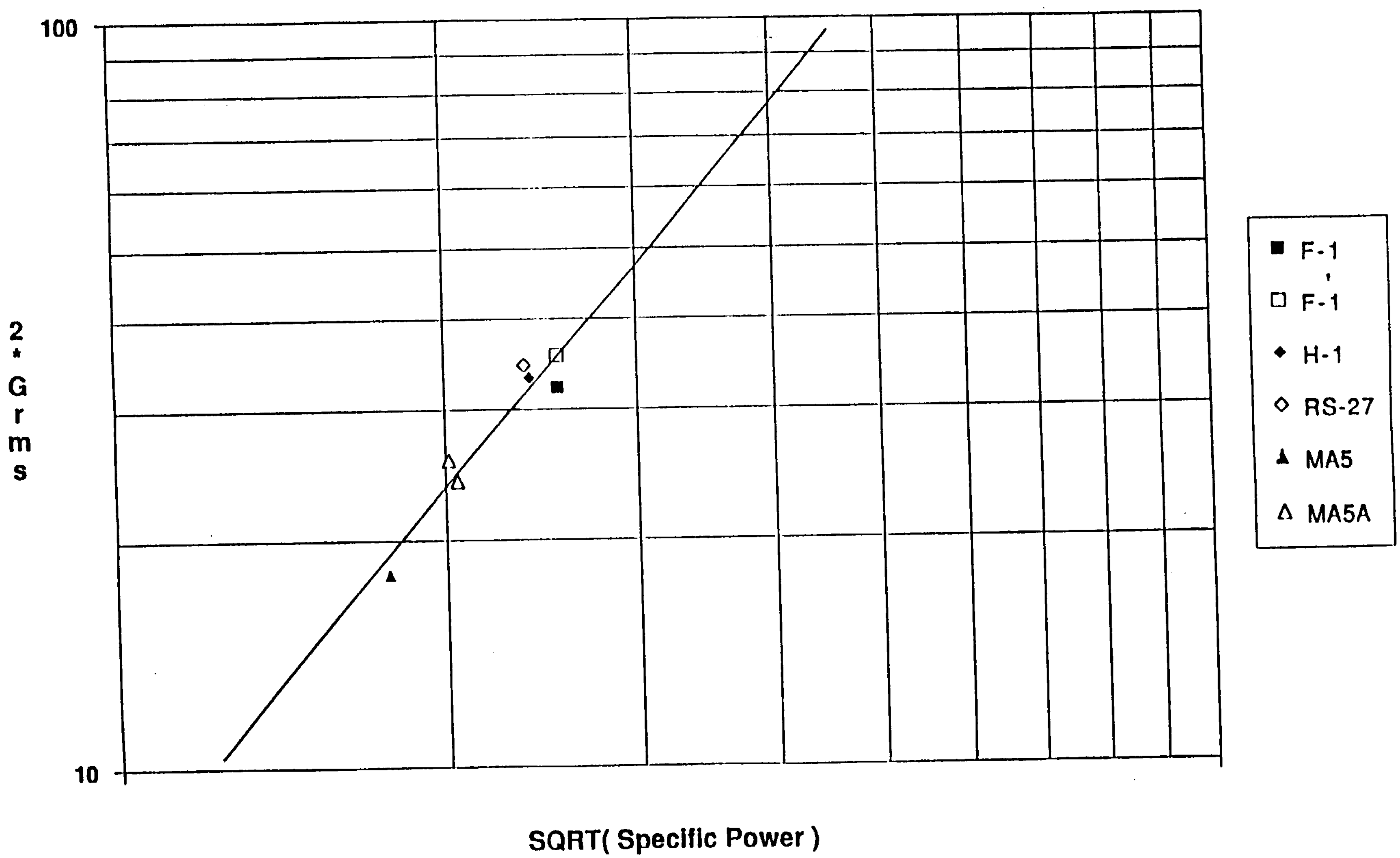

where

G^2_{rms} = Vibrational Power
Ps = Specific Power

The specific power used in the CLS-CSC is expressed in terms of the volumetric flowrate (Q), a pump geometry lumped parameter (Kf), and the pump mass (M).

$$Ps = \frac{Kf*Q^3}{M}$$

The pump geometry lumped parameter accounts for variations in pump geometry that lead to different levels of fluid turbulent pressure fluctuations throughout the pump. Note, the pump geometry lumped parameter, Kf, assumes a constant density flow,m and the method assumes that the quasi-steady-state fluid power lead to uncorrelated acoustic power in the pump. The power of the uncorrelated acoustic waves can be summed to give the pump vibration characteristics. The pump lumped geometry parameter in integral form is defined as

$$Kf = \frac{\int_{x_o}^{x_1}\left(\frac{1}{A(s)}\right)^3 * \frac{1}{L(s)}\ ds}{\int_{x_o}^{x_1} ds}$$

A stream line path is defined between x_o and x_1; A(s) and L(s) are the cross sectional area to the stream line and a characteristic length perpendicular to the stream line, respectively. Thus, the specific power for device is the product of a constant Kf, and readily accessible variables, Q and M.

V.3.2 COMBUSTION CHAMBERS

Estimation of the vibrational environment of combustion chambers is similar to that for turbopumps and is based on the same relation given in equation V.1. The primary difference is the specific power term used. Currently work has only been done on LOX/RP-1 systems that use a ring style injector that is a combination of like duplets, and showerhead injectors. The specific power term used in the CLS-CSC method is expressed in terms of the mean propellant mass flow rate (dm/dt), the mean propellant density (ρ), the combustion chamber mass (M), and the injector faceplate area (A_{inj}).

$$Ps = \left(\frac{\dot{m}^3}{M * (\rho * A_{inj})^2} \right)$$

Thus the combustion chamber specific power and the vibration estimate are for a combustion chamber has a simple dependence on four radily accessible variables.

REFERENCES

I.1. Newell, J. F., Kurth, R. E. and Ho, H., "Composite Load Spectra for Select Space Propulsion Structural Components, Annual Report," NASA CR-179496, NASA Lewis Research Center, March 1986.

II.1. Ho, H., "The Composite Load Spectra Technology," IL 89-103-1034, Rocketdyne Division, Rockwell International Corporation, August 1989.

II.2. Southwest Research Institute, University of Arizona, Rocketdyne Division of Rockwell International Corporation, and J. B. Dias, "Probabilistic Structural Analysis Methods for Select Space Propulsion System Components (PSAM)," NASA Contract NAS3-24389, Annual reports, 1985-1989.

II.3. Coates, R. H., "SSME Phase II Influence Coefficients," SSME 87-000371, or IL 87-129-252, Rocketdyne Division, Rockwell International Corporation, 2 July 1987.

IV.1. Newell, J. F., Rajagopal, K. R., Ho, H. and Cunniff, J. M., "PROBABILISTIC STRUCTURAL ANALYSIS OF SPACE PROPULSION SYSTEM LOX POST", the AIAA 31st Structure, Structural Dynamics, and Materials Conference, Long Beach, CA, April 1990.

IV.2. Romine, W. D., "Main Injector LOX Post Thermal Distribution for the Load Shape Simulations Study", ATU 87-5218, Rocketdyne Division, Rockwell International Corporation, September 1987.

V.1. Roy, D., "A Deterministic Approach to Wall-Pressure Fluctuation in a Complex Engine Ducting System", presented at CLS meeting with NASA, July, 1989.

V.2. Laganelli , A. L., Martenelli, A., and Shaw, L. L., "Wall Pressure Fluctuations in Attached Boundary-Layer Flow", AIAA Journal, Vol. 21, No. 4, 1983.

V.3. Tim Hanshaw and Ben Gutierrez, "Generalized Unsteady Fluid Pressure Propagation Algorithm", IL 0128-0067, Rocketdyne Division, Rockwell International Corporation, 23 May 1990.

V.4. Roland Szabo and Ben Gutierrez, "Pressure Fluctuations in Pipe Bends", IL 0128-0066, Rocketdyne Division, Rockwell International Corporation, 18 February 1991.

V.5. Roland Szabo, "Resultant Forces Due to Separated Flow and Turbulence in the Bends of the SSME LPFP Discharge Duct", SSME 91-1372, or IL 1128-0040, Rocketdyne Division, Rockwell International Corporation, 7 March 1991.

V.6. M.K.Bull and M.P.Norton, "On the Hydrodynamic and Acoustic Wall Pressure Fluctuations in a Turbulent Pipe Flow due to a 90 degree Mitre Bend", Journal of Sound and Vibration, Volume 76, Number 4, Pages 561-586, 1981.

V.7. Sharma, L., "EMPP Task 61908 (Dynamic Environment Definition in Ducts with Bends, Elbows and Manifolds)", Progress Report for February-September 1989, Rocketdyne Division, Rockwell International Corporation, 1989.

V.8. Ito, H., "Pressure Losses in Smooth Pipe Bends", Journal of Basic Engineering, pages 131-143, March 1960.

V.9. Sharma, L., "Transfer Duct Pressure Fluctuations and Correlation Lengths for the Composite Load Spectra Program", SSME-87-1756 or IL SA87-215, Rocketdyne Division, Rockwell International Corporation, December 1987.

V.10. Sharma, L., "HPOP Discharge Duct Pressure Fluctuations and Correlation Lengths for the Composite Load Spectra Program", SSME-87-1757 or IL SA87-216, Rocketdyne Division, Rockwell International Corporation, 4 December 1987.

V.11. Clinch, J. M., "Measurements of the Wall Pressure Field at the Surface of a Smooth-Walled Pipe Containing Turbulent Water Flow", Journal of Sound and Vibration, Volume 9, Number 3, Pages 398-419, 1969.

V.12. Willmarth, W. W., "Pressure Fluctuations Beneath Turbulent Boundary Layers", Annual Review of Fluid Mechanics, Volume 7, Pages 13-38, 1975.

V.13. Bull, M. K. and Norton, M. P., "The Proximity of Coincidence and Acoustic Cut-off Frequencies in Relation to Acoustic Radiation from Pipes with Disturbed Internal Turbulent Flow", Journal of Sound and Vibration, Volume 69, Number 1, Pages 1-11, 1980.

V.14. Barrett, R. E., "Techniques for Predicting Localized Vibratory Environments of Rocket Vehicles", NASA Technical Note D-1836, 1964.

V.15. Harvey, S. A., "MCC Vibration Level Estimation For RSX", IL 1128-0001, Rocketdyne Division, Rockwell International Corporation, January 1991.

APPENDIX A

COMPOSITE LOAD SPECTRA LOAD EXPERT SYSTEM
LDEXPT VERSION 3.0

USER'S MANUAL

Composite Load Spectra

The objective of the composite load spectra is to develop generic load models to simulate the composite load spectra that are induced in space propulsion system components, representative of Space Shuttle Main Engines (SSME), such as transfer ducts, turbine blades, liquid oxygen (LOX) posts and the high pressure oxidizer turbopump (HPOTP) discharge duct.

A knowledge-based system approach is taken to develop the software for this project. This approach provides an environment that facilitates modular and incremental development. It provides links for coupling of symbolic processing and numeric processing. An intelligent database paradigm that coupled a database system with decision trees was implemented on the CLS load expert system. Text knowledge on the databases and associated queries can be assessed inside a decision tree and communicated to users during a consultation session. With the intelligent database paradigm, the system can properly manage the large volume of engineering data and load information that are required for the load spectra synthesis.

The CLS load expert system LDEXPT as shown in Figure 1 has two main modules: the knowledge base module and the rule base module. The functions of the knowledge base module are the database management (DBMS), the duty-cycle-data processing (PROFDP) and the knowledge base system I/O (KBIO). The functions of the rule base module are the expert system consultation task processing (Rule Modules), the user interface with the rule base tools (Rule Base Tools), and the load simulation (ANLOAD).

DBMS

The database management system is a genuine database system. It facilitates the building and maintenance of engine data and knowledge databases. It provides uniform procedures for data and information storage and retrieval. Its usage benefits in avoidance of data redundancy and maintenance of data integrity.

Indexed databases can be built with a maximum of 15 fields and a maximum of 10 keys. Each database record can be retrieved based on its unique key value(s). The maximum number of records in a database is 100. The databases are stored in a knowledge base file by the KBIO module. One database is moved in-core at a time and all database operations are carried out with the in-core database.

The command that activates the database system is ?DBMS. The available commands of the database system are listed below:

Figure 1.

Composite Load Spectra Technology

CLS LOAD EXPERT SYSTEM LDEXPT V3.0

CODE ARCHITECTURE

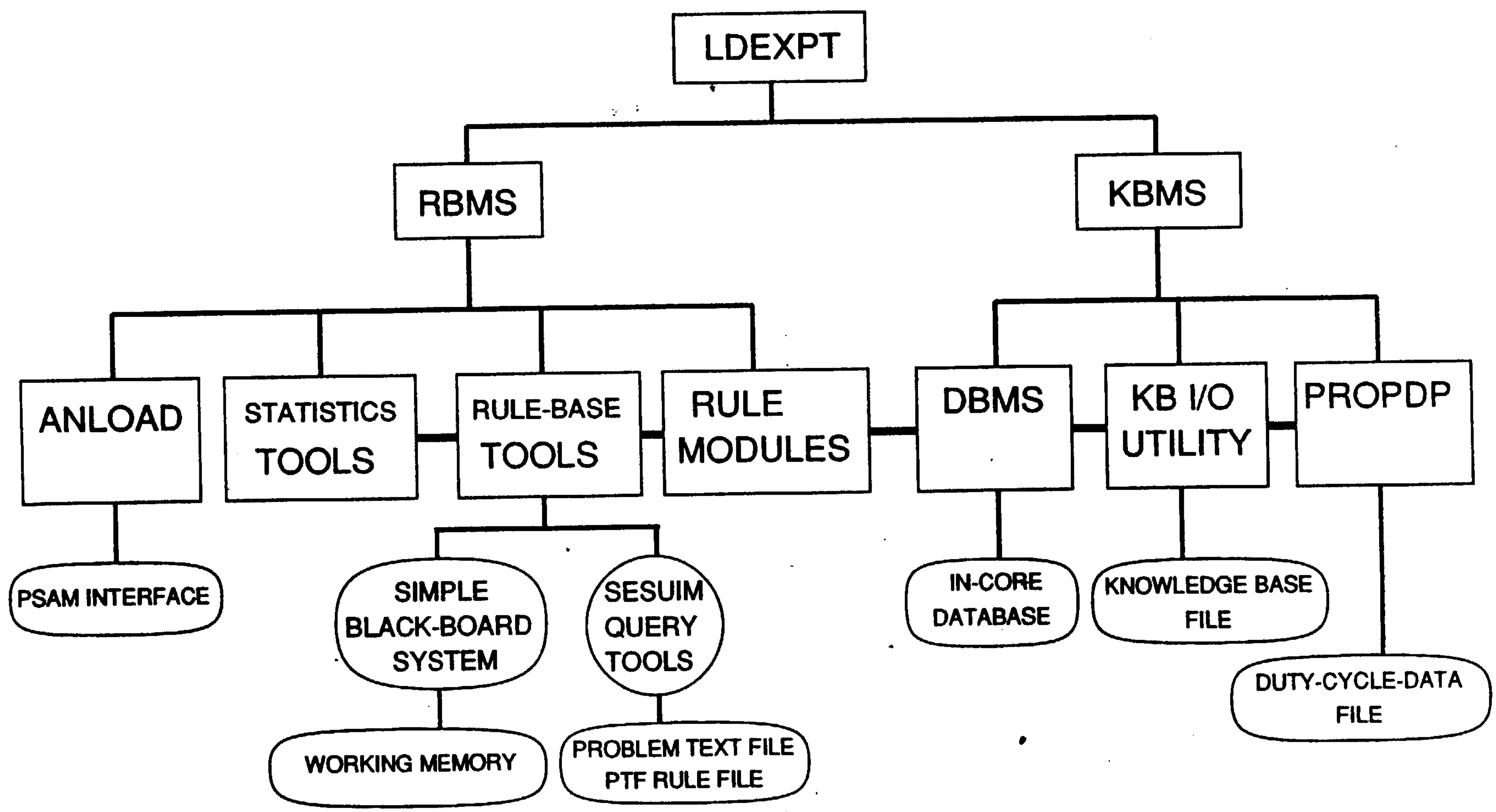

Command	Function
?DBCR	Create a database
?DBCF	Create fields of a database
?DBBK	Build a database key file
?DBSL	Select database record(s)
?DBDL	Delete database record(s)
?DBDF	Display fields and key names
?DBUP	Update or add database records
?DBRD	Open a knowledge base file and read its dictionary
?DBSV	Save a database
?DBLT	List all database records
?DBLK	List key values of all database records
?DBCP	Copy a database to another knowledge base file
?INLD	Input load ID's and Properties from an engine influence model data file
?INFL	Input influence coefficient set from an engine influence model data file
?HELP	List available commands to screen
?RETN	Return to knowledge base driver (KBMS)
?QUIT	Exit the load expert system LDEXPT

PROFDP

PROFile Data Processing (PROFDP) is a duty-cycle-data processing module. It is used to store (to a file) and retrieve engine mission data in piecewise linear form. The mission data for either a test or a flight includes duty cycle power profile, fuel inlet pressure and liquid oxygen (LOX) inlet pressure, etc.

KBIO

KBIO is the Knowledge Base Input/Output module. Its main function is to retrieve a database from the knowledge base file into in-core memory, and to save a database to the knowledge base file when it is created or updated. Both the DBMS and PROFDP modules use the I/O routines of KBIO to precess the files.

The knowledge base file where the databases are stored is a direct access file so that updating of the databases is possible. The KBIO routines were originally written for sequential file operation. Although the routines were adopted to run direct access files, most the operations are still in a sequential file mode. In the next version of LDEXPT, modification will be made to the routines to operate more in tune with the direct access mode.

Rule Modules and Rule Base Tools

Rule modules are routines, each of which performs a certain consultation or data retrieval tasks. Each routine is a decision tree that can interface with user using the rule base query tool. Some rule modules can also call on other modules to perform the required tasks. The query panels presented to users on screen are stored in the problem text file and retrieved with the query tool. A query panel usually consists of knowledge about a database and an associated query. The query panels are activated by a "token", most the time it is associated with a key word of the database.

The rule module tasks consist of the following categories: (1) retrieval of load information and data; (2) engine system and component load model simulations; and (3) preparation of an input file for a mission load simulation. The available rule modules are:

for load information retrieval

- SLIDPL : Independent load information
- SLDEPL : Dependent load information
- SLICGN : Influence coefficient set and gain values
- SLTBCL : Turbine blade component pressure load information
- SLTHCL : Component load information
- SLSCTH : Component thermal load influence model information
- SLICTH : Component thermal load influence coefficients
- SLCLFP : Component fluctuation pressure load information
- SLDUCT : Duct geometry information for fluctuation pressure loads
- SLDDYN : Duct dynamic load PSD information
- SLDCD : Duty-cycle-data profiles information

for engine system and load simulation

- QLM : Quick-Look Model, Gaussian probabilistic engine system load simulation
- SICM : Deterministic engine system influence model load simulation
- STBSM : Simple turbine blade scaling model
- FPSM : Duct fluctuation pressure scaling model

for preparation of mission load simulation input file

- ANLDIN : Preparing ANLOAD (probabilistic load simulation module) input file

KNOWLEDGE DOMAIN

The knowledge domain for the CLS probabilistic load simulations of space propulsion system components consists of complex space propulsion system components and loads information, large volume of engine variable data and engine flight and test mission history data (duty-cycle-data profile), and sophisticated probabilistic methodology and numeric computation for load simulations. A good knowledge representation that facilitates the assess of the load information and data and a suitable development environment that facilitates the coupling of the symbolic process and the numeric process are vital to the development of the CLS knowledge-based system.

For load information and load data, database format is used as their knowledge representation. This representation facilitates the retrieval of load data and model parameters which are critical to load simulation tasks. The load knowledge base for the CLS knowledge-based system LDEXPT version 3.0 as shown in Figure 2 includes three categories of engine loads and variables: (1) Engine inlet conditions and hardware parameters (primitive variables or independent loads); (2) Engine system performance variables and operating condition loads (dependent loads); and (3) Component loads consisting of component internal loads, component environment and local variables. The up-to-date knowledge base has 64 primitive variables as listed in Table 1 and 99 system dependent variables as listed in table 2, and various component loads for four components -- the turbine blade, the LOX post, the HGM transfer ducts and the HPOTP discharge duct. Not all component loads of these four components are implemented. Development of flow related load model and vibration load model are in progress and their related loads will be implemented to the knowledge base when available.

Figure 2.

Composite Load Spectra

Load Expert System Version 3.0
Load Model Knowledge Base

Independent Loads

- Commanded power level
- Engine operating parameters
  - Mixture ratio
  - Fuel inlet pressure & temperature
  - Oxidizer inlet pressure & temperature
- Engine hardware parameters
  - Pump efficiency
  - Turbine efficiency
  - Main oxidizer valve resistance
  - Turbine flow coefficient
- total of 64 independent loads

System Level Dependent Loads

- Engine performance parameters
  - Engine fuel flowrate
  - Engine oxidizer flowrate
  - Engine thrust
- Engine operating parameters
  - Pump speed
  - Turbine inlet & discharge pressures
  - Turbine torque
  - HGM fuel inlet pressure
- Total of 99 dependent loads

Component Level Composite Loads

- Component loads
  - HPFTP turbine blade pressure & temperature
  - Transfer duct static pressure
  - Transfer duct dynamic pressure
  - LOX post temperature
- Local independent loads
  - Coolant seal leakage
  - Hot gas seal leakage
- Composite loads for
  - Turbine blades
  - Transfer ducts
  - LOX posts
  - HPOTP discharge duct

Rockwell International
Rocketdyne Division

89o-4-339-30

TABLE 1. ENGINE INFLUENCE MODEL INDEPENDENT LOADS

ID	INDEPENDENT LOAD	NOMINAL VALUE	C.O.V.
1	Commanded mixture ratio	6.0	0.002
2	Fuel inlet pressure (psia)	30.0	0.259
3	Oxidizer inlet pressure (psia)	100.0	0.327
4	Fuel inlet temperature (R)	37.0	0.016
5	Oxidizer inlet temperature (R)	164.0	0.011
6	Fuel pressurant flowrate (lbm/sec)	0.7	0.0065
7	Oxidizer pressurant flowrate (lbm/sec)	1.5968	0.015
8	HPFP cavitation (%)	1.0	0.001
9	LPFP cavitation (%)	1.0	0.001
10	LPOP cavitation (%)	1.0	0.001
11	Nozzle, mixer delta P (%)	1.1455	0.001
12	MCC throat diameter (in)	10.293	0.001
13	Nozzle exit diameter (in)	90.324	0.001
14	LPFT nozzle area (in^2)	0.95	0.1
15	LPOT nozzle area (in^2)	1.386	0.1
16	LPFP efficiency (%)	1.11	0.0017
17	HPFP efficiency (%)	1.00	0.008
18	LPFT efficiency (%)	1.025	0.0027
19	HPFT efficiency (%)	1.0355	0.01
20	LPOP efficiency (%)	1.14	0.005
21	HPOP efficiency (%)	1.02	0.004
22	PBP efficiency (%)	1.022	0.0016
23	LPOT efficiency (%)	1.022	0.02
24	HPOT efficiency (%)	1.0152	0.01
25	HPOP cavitation (%)	1.0	0.001
26	LPFP head coefficient (%)	0.99	0.007
27	HPFP head coefficient (%)	1.0237	0.008
28	LPOP head coefficient (%)	1.0	0.013
29	PBP head coefficient (%)	1.155	0.004
30	MCC OX dome resistance	0.0384	0.02
31	HGM OX side resistance	0.0032	0.05
32	HGM fuel side resistance	0.0275	0.05
33	MCC Hot Gas injector resistance	0.0031	0.025
34	HGM coolant OX side resistance	0.1040	0.025
35	LPOP disch duct resistance	0.0021	0.01
36	Primary faceplate resistance	15.0	0.075
37	Secondary faceplate resistance	11.17	0.075
38	LPFT seal resistance	7283.0	0.001
39	HPOT coolant circuit resistance	2066.0	0.001
40	HPFP disch duct resistance	0.0123	0.01
41	Main fuel valve resistance	0.0138	0.064
42	Main oxidizer valve resistance	0.0107	0.064
43	MCC OX injector resistance	0.0602	0.025
44	MCC cooling jacket delta pressure	1.031	0.001

TABLE 1 (cont's)

ID	INDEPENDENT LOAD	NOMINAL VALUE	C.O.V.
45	OPB fuel injector resistance	0.685	0.01
46	FPB fuel injector resistance	0.155	0.01
47	LPFT disch duct resistance	0.104	0.01
48	LPFT inlet duct & F-7 resistance	0.5689	0.01
49	PBP inlet duct resistance	0.134	0.01
50	Coolant control valve resistance	0.05568	0.088
51	Baffle flow coefficient	0.95	0.001
52	PB fuel supply duct resistance	0.0071	0.01
53	Nozzle delta P (%)	0.6889	0.001
54	HPOTP turb-end bearing coolant res	65000.0	0.001
55	MCC combustion efficiency (MCC C*)	1.0004	0.001
56	Nozzle heat load (%)	0.884	0.001
57	MCC chamber heat load (%)	0.7932	0.001
58	HPFT flow coefficient	1.0125	0.01
59	HPOT flow coefficient	0.9741	0.01
60	Preburner combustion efficiency (%)	0.98	0.001
61	Mixer delta P (%)	1.0	0.001
62	LOX flow constant (c2)	2.8952	0.001
63	MCC pc measurement error (%)	1.0	0.001
64	Engine fuel flowmeter error (%)	1.0	0.001

TABLE 2. ENGINE INFLUENCE MODEL DEPENDENT LOADS

ID	DEPENDENT LOAD	NOMINAL VALUE	C.O.V.
1	Engine altitude thrust (lbf)	471067.522	0.005
2	HPOTP speed (rpm)	27239.145	0.008
3	HPFTP speed (rpm)	34517.69	0.008
4	HPOP disch pressure (psia)	1595.403	0.0089
5	PB pump disch pressure (psia)	7185.46	0.0098
6	HPFP disch pressure (psia)	6161.829	0.009
7	OPB chamber pressure (psia)	5039.427	0.0129
8	FPB chamber pressure (psia)	4876.04	0.0137
9	Engine oxidizer flowrate (lbm/sec)	894.34	0.0062
10	Engine fuel flowrate (lbm/sec)	149.06	0.0069
11	Oxidizer pressurant flowrate(lbm/sec)	1.5968	0.015
12	Fuel pressure flowrate (lbm/sec)	0.6996	0.0065
13	OPB oxidizer valve position (%)	0.6495	0.0147
14	FPB oxidizer valve position (%)	0.7652	0.0135
15	MCC oxidizer injector pressure(psia)	3540.82	0.0086
16	MCC Hot Gas injector pressure (psia)	3237.36	0.0064
17	MCC injector end pressure (psia)	3006.0	0.0058
18	HPOP inlet pressure (psia)	380.07	0.0228
19	HPFP inlet pressure (psia)	226.084	0.0263
20	HPOP disch temperature (R)	190.195	0.002
21	HPFP disch temperature (R)	94.904	0.0114
22	MFV disch temperature (R)	95.491	0.0114
23	PB pump disch temperature (R)	203.377	0.0025
24	HPOP inlet temperature (R)	169.425	0.006
25	HPFP inlet temperature (R)	42.472	0.0019
26	LPOTP speed (rpm)	5042.8	0.008
27	LPFTP speed (rpm)	15850.64	0.0087
28	HPOT disch temperature (R)	1352.533	0.0274
29	HPFT T/D disch temperature (R)	1625.723	0.0193
30	OPB oxidizer valve resistance	130.79	0.098
31	FPB oxidizer valve resistance	13.18	0.15
32	Oxidizer pressurant pressure (psia)	3439.598	0.0092
33	Fuel pressurant pressure (psia)	3348.296	0.0079
34	Oxidizer pressurant temperature (R)	838.0	0.0245
35	LPFT disch temperature (R)	472.95	0.0125
36	LPOP suction specific speed (NSS)	8054.341	0.02
37	LPFP suction specific speed (NSS)	19738.26	0.02
38	HPOP suction specific speed (NSS)	11295.08	0.0185
39	HPFP suction specific speed (NSS)	6017.04	0.024
40	MCC coolant disch pressure (psia)	4840.48	0.0108
41	LPOT torque (ft-lbf)	1565.124	0.0159
42	LPFT torque (ft-lbf)	996.605	0.0182
43	HPOT torque (ft-lbf)	4436.78	0.0108
44	HPFT torque (ft-lbf)	9452.388	0.0142

TABLE 2 (cont's)

ID	DEPENDENT LOAD	NOMINAL VALUE	C.O.V.
45	LPOT flowrate (lbm/s)	176.17	0.01
46	LPFT flowrate (lbm/s)	26.46	0.0175
47	HPOT flowrate (lbm/s)	58.95	0.01
48	HPFT flowrate (lbm/s)	158.92	0.0107
49	LPOT inlet pressure (psia)	3947.348	0.0895
50	LPFT inlet pressure (psia)	4508.63	0.0105
51	HPOT inlet pressure (psia)	5019.85	0.00875
52	HPFT inlet pressure (psia)	4857.17	0.0095
53	LPOT inlet temperature (R)	190.195	0.002
54	LPFT inlet temperature (R)	489.121	0.0122
55	HPOT inlet temperature (R)	1501.062	0.0266
56	HPFT inlet temperature (R)	1812.757	0.0186
57	LPOT disch pressure (psia)	414.28	0.0208
58	LPFT disch pressure (psia)	3403.035	0.0076
59	HPOT disch pressure (psia)	3318.146	0.0066
60	HPFT disch pressure (psia)	3439.885	0.0067
61	LPOT power (bhp)	1502.269	0.024
62	LPFT power (bhp)	3013.01	0.027
63	HPOT power (bhp)	23012.439	0.0155
64	HPFT power (bhp)	62192.2	0.0175
65	HGM inlet pressure, fuel (psia)	3356.87	0.0075
66	HGM inlet pressure, OX (psia)	3302.345	0.0075
67	Oxidizer T/D dynamic pressure (psia)	16.6	0.01
68	Oxidizer T/D flow velocity (ft/s)	454.81	0.01
69	Fuel T/D dynamic pressure (psia)	25.72	0.01
70	Fuel T/D flow velocity (ft/s)	578.4	0.01
71	HPOT mixture ratio (O/F)	0.7323	0.034
72	HPFT mixture ratio (O/F)	0.9267	0.0227
73	OPB power (bhp)	168661.0	0.02
74	FPB power (bhp)	544895.0	0.02
75	MCC power (bhp)	1.2473E+07	0.005
76	OPB OX in manifold pressure (psia)	5927.91	0.013
77	OPB fuel in manifold pressure (psia)	5360.543	0.0085
78	FPB OX in manifold pressure (psia)	6088.94	0.0137
79	FPB fuel in manifold pressure (psia)	5400.416	0.0088
80	PBP disch, PB OX supply temp (R)	203.377	0.0025
81	Mixer disch, PB fuel supply temp (R)	275.777	0.0045
82	Fuel HGM velocity (ft/s)	1322.532	0.01
83	Fuel HGM dynamic pressure (psia)	132.983	0.01
84	LOX HGM velocity (ft/s)	214.13	0.01
85	LOX HGM dynamic pressure (psia)	3.737	0.01
86	OPB fuel dynamic pressure (psia)	0.1978	0.01
87	OPB fuel flow velocity (ft/s)	367.214	0.01
88	FPB fuel dynamic pressure (psia)	44.647	0.01

TABLE 2 (cont's)

ID	DEPENDENT LOAD	NOMINAL VALUE	C.O.V.
89	FPB fuel flow velocity (ft/s)	411.96	0.01
90	HPOP disch dynamic pressure (psia)	230.658	0.01
91	HPOP disch velocity (ft/s)	174.213	0.0052
92	HPOP head rise (ft)	7545.048	0.0095
93	HPFP disch dynamic pressure (psia)	123.277	0.01
94	HPFP disch velocity (ft/s)	469.11	0.0055
95	HPFP head rise (ft)	174050.04	0.0085
96	PBP disch dynamic pressure (psia)	32.48	0.01
97	PBP disch velocity (ft/s)	65.14	0.0052
98	HGM coolant inlet pressure (psia)	3346.037	0.0074
99	Engine nozzle exit velocity (ft/s)	14562.83	0.01

Engine model and component load models are needed to evaluate the simulated probabilistic loads. A multi-level engine model that couples the engine model with various component load models was implemented to correlate component loads with the engine performance variables and engine (hardware and inlet conditions) primitive variables. The CLS load models implemented are as listed in Figure 3: the engine system model is a probabilistic influence model, various component load models including the generic static pressure scaling model, the generic probabilistic thermal load model, various turbine blade load scaling models, and LOX post transient thermal load model. Load simulation routines were developed for these load models and implemented in the load simulation module ANLOAD. Generic load models were developed whenever possible so that they could be applied to different system components without remodeling the load again. In such cases, the component specific data and information of the component loads are stored in the knowledge base. These component specific information will be retrieved and supplied to the generic model when the component load is evaluated.

The knowledge base file has the following databases:

- LIDP : Engine primitive variables or independent loads
- LDEP : Engine system dependent variables or loads
- INFC : Engine influence model coefficient set
- LTBC : Turbine blade pressure scaling model
- DFAT : Engine flight and test data information
- LCTH : Component loads
- SCTH : Component load and boundary load scaling models
- ICTH : Component load and boundary load influence coefficients
- CLFP : Component fluctuation pressure load parameters
- DUCT : Duct geometry zones

Detail description of the databases is presented in Appendix A.1.

ANLOAD

ANLOAD is the load simulation module that performs mission simulations of the probabilistic system and component loads. ANLOAD was linked to RBMS, the driver of the Rule Base module, and it can be executed with the command ?ANLD. However, ANLOAD is an independent module. It could be easily made into a stand-alone load simulation program. An input file INFILE DAT is required to run ANLOAD. All load information and engine data are supplied to ANLOAD with the INFILE. This illustrates the loosely coupling scheme of coupling the symbolic processes and the numeric processes employed in the CLS system. The consultation rule module RBTBIN interfaces with the user and prepares an input file for the user's load simulation task. The only connection of the load simulation (a numeric process) module is through the input file. The detail descriptions of input variables and input format are presented in Appendix A.2.

Figure 3.

Composite Load Spectra

Load Expert System Version 3.0
Load Model Knowledge Base

Engine System Model

- Load distributions
  - Means
  - Coefficients of variation
  - Distribution types
  - Nominal value coefficients
- Probabilistic influence model
  - Influence coefficients
  - 1 σ gain values

Component Load Models

- Generic static pressure scaling model
- Generic probabilistic thermal load model
- Generic turbine blade pressure load model
  - Tip, mean & hub cross section pressures
  - Turbine blade pressure interpolation scheme
- HPFTP 2nd stage turbine blade pressure & temperature loads
  - 2519 nodes geometry model
  - Reference nodal pressures & temperatures
- Turbine blade dynamic pressure load model
- Duct dynamic pressure load model
  - Transfer ducts, LOX posts, HPOTP discharge duct
- Transient LOX post thermal load model
- Vibration model

Three probabilistic methods implemented in the ANLOAD module are: (1) the Gaussian moment propagation method, (2) the RASCAL (randomized sampling condensation algorithm) method, and (3) the Monte Carlo method. The Gaussian method is the most simple and efficient method. Analytical results can be obtained for the simple cases of load models. This method is most frequently used as an approximation method for a preliminary probabilistic design and analysis. The RASCAL method developed by Dr. R. E. Kurth is a variance of the discrete probabilistic distribution (DPD) method. The method can be applied to models having variables with arbitrary (non-analytical) distribution function. The method is fairly accurate and efficient. It is assigned as the default method for CLS load simulations. The Monte Carlo method is the most versatile and accurate method. It can be applied to any load models. With the rapid increase of computing power per dollar every year, computing cost of the Monte Carlo method is becoming less of a problem.

The ANLOAD load calculation process is shown in Figure 4. At each time step, ANLOAD first calculates the relevant system dependent variables and loads using the engine influence model. Next, it evaluates the component loads with various complexity dependent of the load models. If a complete mission simulation is requested, the time step will go through the input mission history profile from start transient state, to the steady state and then to the engine cutoff transient state. ANLOAD is doing a good job in load simulation during the steady state because the engine influence model and the component load models were mostly developed for the steady state. The generic model for all system loads with a few exceptions during transient states (start and cutoff) is the pseudo-steady-state model. This model assumes that during each time step of the transient states, the loads are treated as though they are in steady state with constant coefficient of variation through out the transient. The few exceptions are those system loads such as the high pressure fuel turbine inlet temperature that experience spike during the start transient. The empirical mean spike transient functions of these loads are stored in a routine of transient load object functions and will be activated when those loads are simulated. The transient component loads are treated individually as they are implemented to the CLS knowledge-based system.

Figure 4. ANLOAD FLOWCHART

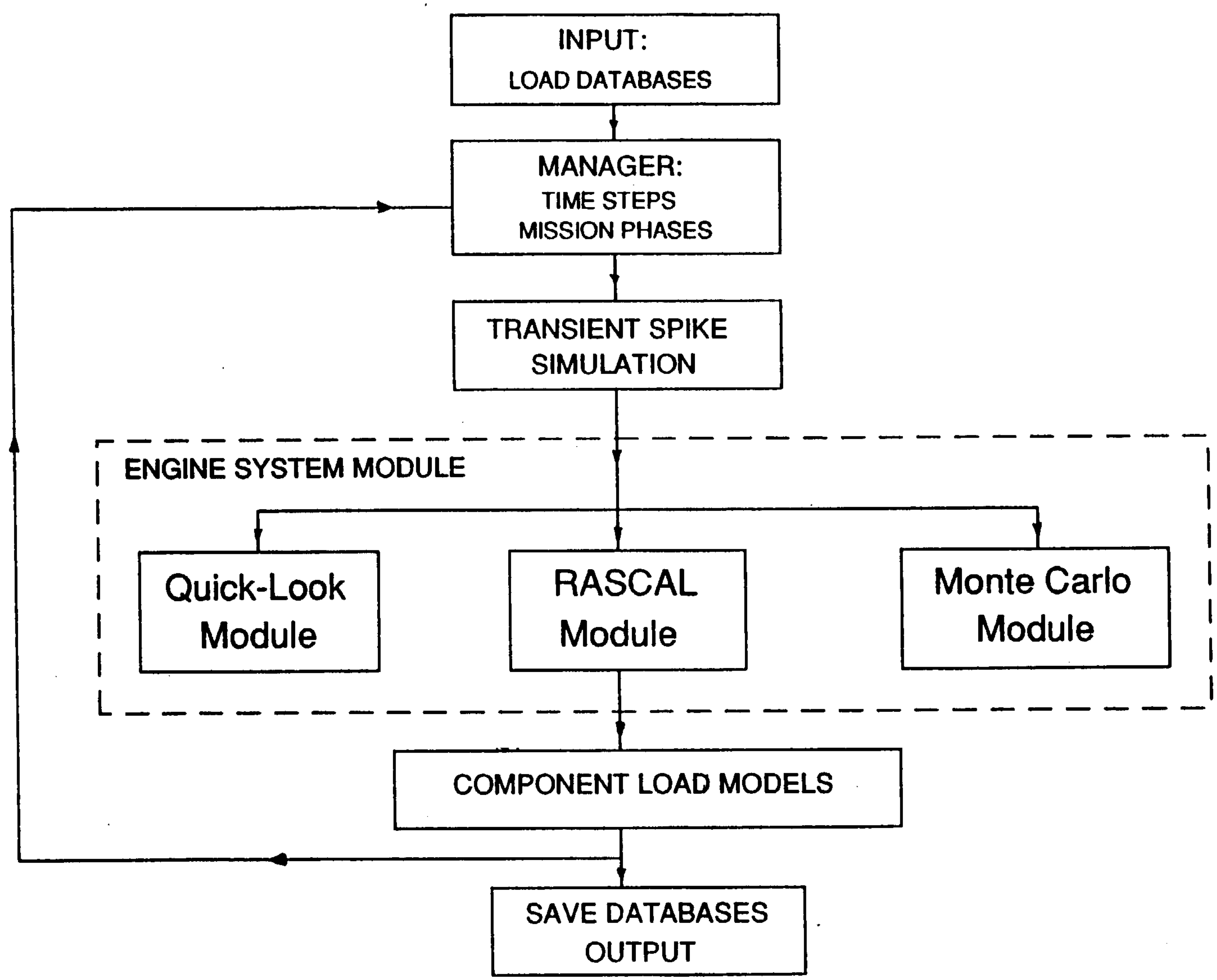

LDEXPT OPERATION

The load expert system, LDEXPT version 3.0, was installed on the NASA/LeRC's VM system. Its function is to synthesize the rocket engine component load spectra.

I. START THE LOAD EXPERT SYSTEM

To run the expert system, one needs
(1) Request more virtual memory by executing a CP command:

    CP DEFINE STORAGE 5026K

(2) Returns to the CMS:

    CP IPL CMS

(3) Loading the graphic-3D package:

    GRAPH3D

(4) Loading the load expert system:

    LDEXPT

The LDEXPT command sets up the required files, loads the program and start running the program.

II. THE LOAD EXPERT SYSTEM CONSULTATION

To run an expert system consultation session

(1) Enter ?RBMS command to go to RBMS. A menu listed the available commands will appear.

(2) Enter ?EXDR command to start the consultation. A list of rule modules will appear on screen:

```
SLIDPL : Retrieve Independent Load Information
SLDEPL : Retrieve Dependent Load Information
SLICGN : Retrieve Influence Coefficients and Gains
SLTBCL : Retrieve Turbine Blade Component Pressure Load
         Scaling Model Information
SLDCD  : Retrieve and Plot a Duty-Cycle-Data profile
SLTHCL : Retrieve Component Thermal Load Information
SLSCTH : Retrieve Thermal Load Scaling Model and Influence
         Model Information
SLCLFP : Component fluctuation pressure load information
SLDUCT : Duct geometry information for fluctuation pressure
         loads
SLDDYN : Duct dynamic load PSD information
QLM    : Quick Look Model for Evaluating Dependent Load
SICM   : Deterministic Influence Coefficient Model
STBSM  : Simple Scaling Model for Evaluating the Turbine
         Blade Component Pressure Load
ANLDIN : Prepare ANLOAD (probabilistic load simulation) input
         file
EXIT   : Exit the Expert System Driver
```

Select one of the module, e.g. QLM, the expert system will start the session.

III. THE LOAD CALCULATION

To run the full scale load spectra calculation, one needs to run the ANLDIN rule module to prepare an ANLOAD input file or prepare one manually. Then EXIT the expert system driver and back to the RBMS subsystem. Enter ?ANLD, the ANLOAD module (the load calculation module) will start running.

IV. THE DATABASE SYSTEM

The database system is a simple flat file system. It has all the basic database operations such as creating a database, inserting and deleting a database record, etc.

To go to the database system, enter ?DBMS at the KBMS menu prompt. A list of database commands will appear on screen:

```
?DBCR : Create a database table
?DBCF : Create fields for a database
?DBBK : Build key data
?DBSL : Select database record(s)
?DBDL : Delete database record(s)
?DBDF : Display field and key names
?DBUP : Update (Add) database record(s)
?DBRD : Open a database file
?DBSV : Save an updated database
?DBLT : List all of a database's records
?DBLK : List all key variables of a database
?DBCP : Copy a database to another knowledge base file
?INLD : Input load ID & properties
?INFL : Input influence coefficients
?HELP : List available database commands
?RETN : Return to KBMS
?QUIT : Exit LDEXPT
```

(1) Open an existing database

To work with an existing database, one needs first to open the database file by entering ?DBRD. Then, one can proceed to select a database record, update a database record, etc. by entering an appropriate command, e.g. ?DBSL, the system will carry out the desired database task.

The ?INLD and ?INFL commands are not generic database functions. They are provided for the composite load spectra project to build the load knowledge base.

(2) Create a new database

To create a new database, one needs to run the command ?DBCR to define the database field names and their attributes. After that, the system will prompt you to enter the database records.

When all database records are entered, one needs to run the command ?DBBK to build a key index file.

After building the index file, one can perform other operation on the new database. Before leaving the database system, the last step is to run ?DBSV to save the database to the knowledge base file.

(3) Create rocket engine influence model databases

The CLS load expert system LDEXPT should have already the SSME influence model databases stored on the knowledge base file. The commands ?INLD and ?INFL are included for the system programmers who need to update a complete set of influence model databases or build a new set of influence model databases for a different type of rocket engines.

To build a new set of influence model databases, one needs to have an influence coefficient file following the influence coefficient file format of the Rocketdyne system performance and analysis group. The influence coefficient file essentially has three groups of data. The first group is a list of engine primitive variables or independent loads with format of (2I6,4E12.5). The data supplied for this group are:

```
ID,IDUM,(ANOM(j),j=1,4)
```

where, ID is the independent load ID,
IDUM is not used,
ANOM(j)'s are the nominal value coefficient set.

The second group is a list of engine performance variables and system operating loads, or system dependent loads. The format is the same as the first group, (2I6,4E12.5). The data are:

```
ID,IDUM,(ANOM(j),j=1,4)
```

where, ID is the dependent load ID,
IDUM is not used,
ANOM(j)'s are the nominal value coefficient set.

The third group is a list of engine influence coefficient set. The format is (3I4,4E12.5). The data are:

```
ID(i),JD(j),KDUM,(CINF(i,j,jj),jj=1,4)
```

wqhere, ID(i) is the ith independent load
JD(j) is the jth dependent load
KDUM is not used
CINF(i,j,jj)'s are the influence coefficient set

With the influence coefficient data file, one can build the engine influence model databases. The first step is to build the independent loads database. The next step is to build the dependent load database and lastly to build the influence coefficient set database. The procedure is as follows:

(1) Run LDEXPT and go to DBMS module
(2) Enter ?DBCF to define the fields of the independent load database
(3) Enter ?INLD to build the database, choosing option 1 of ?INLD
(4) When step (3) is done, choosing option 3 of ?INLD to exit from ?INLD so that the database is saved.
(5) Exit LDEXPT and make a backup copy of the knowledge base file
(6) Run LDEXPT and go to DBMS module
(7) Enter ?DBCF again to define fields of the dependent load database
(8) repeat steps (3) and (4) for dependent load database
(9) Exit LDEXPT and make another backup copy of the knowledge base file
(10) Enter ?DBCF to define the fields of the influence coefficient set database
(11) Enter ?INFL to build the influence coefficient set database
(12) Exit LDEXPT and make a back up copy of the knowledge base

APPENDIX A.1

CLS LDEXPT DATABASES

KNOWLEDGE BASE INFORMATION

DATABASE LIDP : the system independent load database

LIDP-ID : the independent load ID number
LD-NAME : the independent load name
MEAN : the nominal engine mean value of the load
COV : the coefficient of variation of the load
P3 : rare event probability, not used
DIST : distribution type of the load
NE-COEF1: the constant term coefficient for the nominal engine value calculation
NE-COEF2: the first order term coefficient
NE-COEF3: the second order term coefficient
NE-COEF4: the third order term coefficient

The nominal engine mean value is calculated as a third order polynomial of the control power level T in power unit (i.e. T = 1 is at 100% power level):

MEAN = COEF1 + COEF2*T + COEF3*T*T + COEF4*T*T*T

DATABASE LDEP : the system dependent load database

LDEP-ID : the dependent load ID number
LD-NAME : the dependent load name
MEAN : the nominal engine mean value
COV : coefficient of variation
P3 : rare event probability, not used
DIST : distribution type of the load
NE-COEF1: the constant term coefficient for evaluation of the load's nominal engine mean value
NE-COEF2: the first order term coefficient
NE-COEF3: the second order term coefficient
NE-COEF4: the third order term coefficient

DATABASE INFC : the influence coefficient set and gains database

LDEP-ID : the dependent load ID
LIDP-ID : the independent load ID
INFL-C1 : the constant term coefficient for evaluation of the influence coefficient as a polynomial of third order control power level T in power unit
INFL-C2 : the first order term coefficient
INFL-C3 : the second order term coefficient
INFL-C4 : the third order term coefficient
GAIN65 : the gain of the dependent load at power level of 65% as a result of one sigma change in the independent load
GAIN90 : the gain at 90% power level
GAIN100 : the gain at 100% power level
GAIN104 : the gain at 104% power level

The influence coefficient is calculated the same way as the load nominal engine value:

IC = C1 + C2*T + C3*T*T + C4*T*T*T

and the percentage gain of the dependent load due to the change in the independent load is calculated as follows:

Percent change of Dep. Load = IC * Percent change of Indep. Load

DATABASE LTBC : Turbine Blade Component pressure Load information

TB-C-ID : the turbine blade component ID
TB-LD-ID: the turbine blade load ID number
TB-LD-NA: the turbine blade load name
LD-TYPE : load type
LDEP1-ID: the first dependent load ID used in the scaling model
LDEP2-ID: the second dependent load ID used in the scaling model = 0 means only one dependent load is needed
SC-COEF : the coefficient of the scaling model
TBC-GRPN: group name of the scaling model coefficient data file

DATABASE DFAT : engine flight and test data information

DCD-ID : duty-cycle-data (engine flight or test data) ID
LIDP-ID : the independent load ID of the data
ENGINE : engine type
MISSION : mission history phase
DCD-GRPN: duty-cycle-data group name of the data file

DATABASE LCTH : the component thermal load information

CMPN-ID : the component ID number
C-LD-ID : the component load ID number
C-LD-NA : the component load name
MEAN : the nominal mean value of the load
COV : the coefficient of variation of the load
P3 : not used
DIST : distribution type, assumed to be normal for now
NE-COEF1 : not used
NE-COEF2 : not used
NE-COEF3 : not used
NE-COEF4 : not used

DATABASE SCTH : the thermal load scaling model and influence model database

CMPN-ID	: the component ID number
C-LD-ID	: the component load ID number
C-LD-NA	: the component load name
LD-TYPE	: the load type, it is used to indicate the type of dependency of the load in its influence model e.g. a LD-TYPE of FOURBD means the load needs four boundary loads in its influence model calculation
C1-ID	: component ID of the first dependent load or the first boundary load =0 means it is a dependent load
LDEP1-ID	: the first dependent load ID or the first boundary load ID
C2-ID	: component ID of the second dependent load or the second boundary load
LDEP2-ID	: the second load ID
C3-ID	: the third component ID
LDEP3-ID	: the third load ID
C4-ID	: the fourth component ID
LDEP4-ID	: the fourth load ID
C5-ID	: the fifth component ID
LDEP5-ID	: the fifth load ID
SC-COEF	: the scaling coefficient for a LD-TYPE of ONE case
SC-GRPN	: the scaling coefficient file group name, not used

DATABASE ICTH : the boundary condition load gain database

CMPN-ID	: the boundary condition load component ID
C-LD-ID	: the boundary condition load ID
C1-ID	: the dependent load component ID
LDEP1-ID	: the dependent load ID
GAIN	: the gain coefficient, used as follows

Percent change of the boundary load with C-LD-ID due to LDEP1 = GAIN * Percent change of the dependent load LDEP1

DATABASE CLFP : the fluctuation pressure model parameters database

COMP-ID	:	the component ID
C-L-ID	:	the component load ID
C-L-NA	:	the component load name
LOCATION	:	duct location where C-L-ID is to be evaluated
DIA-EQV	:	equivalent diameter
FI-RATIO	:	fluctuation intensity ratio
CORLEN	:	correlation length
SHAPE-F	:	shape factor
FREQ-0	:	lower bound of the PSD frequency range
FREQ-I	:	intermediate separation point of the PSD
FREQ-L	:	upper bound of the PSD frequency range
A-L-FREQ	:	percentage area for the lower half of the PSD

DATABASE DUCT : duct geometry database

COMP-ID	:	the component ID
C-L-ID	:	the component load ID
N-ZONES	:	number of zones of the component
LOC-1	:	location of zone 1
LOC-2	:	location of zone 2
LOC-3	:	location of zone 3
LOC-4	:	location of zone 4
LOC-5	:	location of zone 5
LOC-6	:	location of zone 6
LOC-7	:	location of zone 7
LOC-8	:	location of zone 8
LOC-9	:	location of zone 9
LOC-10	:	location of zone 10
LOC-11	:	location of zone 11
LOC-12	:	location of zone 12

APPENDIX A.2

ANLOAD INPUT FILE USER'S GUIDE

ANLOAD INPUT FILE can be created either manually or using command ?INPP in LDEXPT. It can use any name in accordance with DOS convention. The input file name will be requested by ANLOAD during runtime. The followings are the format of the input file.

```
Card #1, format(I6)
MODEL
      =1  Gaussian Method
      =2  DPD Method
      =3  Monte Carlo Method
      =9  Marginal Distribution Method
      =11 Marginal Distribution Method treating dependent loads
          and component local loads as input variables

Card #2.1, format(2I6), required if MODEL=2
NBIN,NEND
      NBIN : Number of bins
      NEND : Number of intervals in each bin for the combined
             distribution

Card #2.2, format(I6), required if MODEL=3
NMC
      NMC : Number of Sampling Points

Card #3, format(3E12.5,6X,I6,E12.5)
TFIRST,TLAST,DELTSS,DELTTS,NPRT,FAIL
      TFIRST: Starting time, the first time step to be evaluated
              at the time (TFIRST+DELT)
      TLAST : time for the last time step, i.e. end time
      DELTSS: delta time, i.e. time step size, for steady state
              load calculation used only with the duty-cycle-data
              option
      DELTTS: delta time for transient state load calculation
      NPRT  : Number of time steps between printing
      FAIL  : failure criterion

Card #4, format(I6,A20)
IZERO,NPWR
      IZERO = 0
      NPWR  : power profile name

Card #5, format(I6,2E12.5)
IPWR,PWRO
      IPWR  : POWER options
            = 0  POWER=PWRO
            = 1  POWER=PWRO+PWRATE*TIME
            = 2  POWER input from PFPWR profile
      PWRO  : power constant term
```

```
Card #6.1, format(6E12.5), required if (IPWR.EQ.1)
PWRO,TIMEO,PWR1,TIME1,PWR2,TIME2
      PWRO  : POWER LEVEL AT TIME TIMEO, THIS IS THE FIRST POINT
              OF THE TIME INTERVALS
      TIMEO : TIME OF THE FIRST POINT OF TIME INTERVAL
      PWR1  : POWER LEVEL AT TIME1
      TIME1 : TIME OF THE SECOND POINT
      PWR2  : POWER LEVEL AT TIME2
      TIME2 : TIME OF THE THIRD POINT
              THE LAST POINT OF THE POWER PROFILE IS (PWR2,TLAST)
              THE LAST INTERVAL IS ASSUMED TO BE STEADY STATE
              WHERE POWER STAYS CONSTANT

Card #6.2, format(I6), required if (IPWR.EQ.2)
NPRPWR
      NPRPWR : number of pairs for the power duty-cycle-data
               profile

Card #6.3-6.n, format(6E12.5), required if (IPWR.EQ.2)
PFPWR(I,J), J=1,3; I=1,NPRPWR
      PFPWR(I,1) : time for the ith data point in the profile
      PFPWR(I,2) : power level of the ith data point
      PFPWR(I,3) : power level standard deviation of the ith data
                   point

Card #7, format(I6)
NLOAD
      NLOAD : Number of independent loads
              maximum of 15 is allowed

Card #8.1, format(I6,A20,A4), repeat cards #8 as a set
                  (i.e.#8.1-#8.n) NLOAD times required
                  if (NLOAD <> 0)
IDPID(I),NAME(I),LOADNS(I)
      IDPID(I)  : the ith independent load ID number, see
                  documentation on that or run LDEXPT to find out
                  what they are
      NAME(I)   : the ith independent load name
      LOADNS(I): the ith independent load stationarity
               = 1 non-stationary duty-cycle-data input profile
               = 0 stationary, constant mean and variance

Card #8.2, format(6E12.5), required if (NLOAD <> 0)
CINOM(I,J),J=1,4
      CINOM(I,J): the nominal engine coefficient set
```

```
Card #8.3, format(I6,3E12.5), required if (NLOAD <> 0)
IGO(I),P1(I),P2(I),P3(I)
      IGO(I) : pdf type
             = 0  constant
             = 1  uniform
             = 2  normal
             = 3  lognormal
             = 4  Rayleigh
             = 5  extreme value of type I
      P1(I)  : mean parameter
               for lognormal, it is the LOG(Median)
               for Rayleigh, it is the shifted origin (the left
               boundary)
               for extreme value, it is like the shifted origin
      P2(I)  : variance parameter
               for normal, it is the standard deviation
               for lognormal, the standard deviation of the
               LOG(x) distribution
               for Rayleigh, it is the (Beta/sqrt(2))
               for extreme value, it is the
               Alpha=sqrt(1.645/variance)
      P3(I)  : not used

Card #8.4, format(I6), required if (LOADNS(I) = 1)
NPAIR
      NPAIR : Number of the duty cycle profile data point

Card #8.5, format(6E12.5), required if (LOADNS(I) = 1)
PFILD(K,J), J=1,3; K=1,NPAIR
      PFILD(K,1) : the kth data point for time axis
      PFILD(K,2) : the kth data point for the Ith independent
                   load
      PFILD(K,3) : the kth point for the standard deviation of
                   the Ith independent load

Card #9, format(I6)
NRARE
      NRARE : Number of transient loads or shocks

Card #10.1, format(E12.5,A), required if NTRAN <> 0 and repeat
                             card set (#10.1-#10.n) NRARE times
NAME(II)
      NAME(II): name of the ith shock

Card #10.2, format(2I6,E12.5)
IRARE(II),MPTRN(II),FREQ(II)
      IRARE(II): not used, save for rare event simulation
      MPTRN(II): not used
      FREQ(II) : not used
```

Card #10.3, format(I6,3E12.5)
IGO(II),P1(II),P2(II),P3(II)

- IGO(II) : pdf type of the ith shock
- P1(II) : mean parameter for the ith shock
- P2(II) : variance parameter
- P3(II) : not used

Card #11, format(I6)
NRESP

- NRESP : Number of dependent loads (or response loads)

Card #12.1, format(I6,A20), repeat card set #12 NRESP times
ICOMB(I),NAME(15+I),STATE(I)

- ICOMB(I) : the ith dependent load ID number, see documentation
- NAME(15+I): name of the ith dependent load
- STATE(I) : it is the value of the dependent load for which a limit state probability should be calculated

Card #12.2, format(4E12.5), required if (NRESP <> 0)
ANOM(I,J),J=1,4

- ANOM(I,J): nominal value coefficient set

Card #12.3, format(4E12.5), required if (NRESP <> 0)
(CINF(K,I,J),J=1,4),K=1,NLOAD

- CINF(K,I,J): influence coefficient set the Ith dependent load varied due to the Kth independent load

Card #12.4, format(I6)
IDEP(I)

- IDEP(I) : Number of independent loads whose effect on the ith dependent load are to be evaluated

Card #12.5, format(12I6)
ITEMP(J), J=1,IDEP(I)

- ITEMP(J) : the independent load number as assigned by the order it entered in NLOAD loop

Card #13, format(I6)
NOUT

- NOUT : Number of component loads whose pdf's are to be generated

```
Card #14.1, format(I6), required if (NOUT <> 0) and repeat
                        card set (#11.1-#11.n) NOUT times
ITBCOM(I)
      ITBCOM(I): component options
               = 1  for HPFTP turbine
               = 2  for HPOTP turbine
               = 3  for LPFTP turbine
               = 4  for LPOTP turbine
               = 5  for HGM fuel center transfer tube
               = 6  for LOX post or LOX post region A
               = 7  for LOX post region B
               = 8  for LOX post region C
               = 9  for HPOTP oxidizer transfer duct
               =10  for HPOTP discharge duct

Card #14.2, format(I6,A20)
IBLOAD(I),NAME(IB+I)
      IBLOAD(I)  : the ith component load ID number
      NAME(IB+I): name of the ith component load
                   where IB=NLOAD+NRARE+NRESP

Card #14.3, format(A4)
GRNBLC(I)
      GRNBLC(I)  : the group name of the component load scaling
                   coefficient file, mainly for turbine blade
                   "NULL" if not needed

Card #14.4, format(2I6,E12.5)
ID1(I),ID2(I),C1(I)
      ID1(I)  : first dependent load ID for the ith component
                load, used for turbine blade pressure loads only
                for thermal load, set it equals to zero
      ID2(I)  : second dependent load ID, same usage as above
      C1(I)   : scaling coefficient for the ith component load

Card #14.5, format(I6) required if (GRNBLC(I).EQ.'NULL')
ISD(I)
      ISD(I) = 1 scaling depends on a single dependent load
             = 2 scaling depends on two dependent loads
             = 999 used for thermal load scaling model

Card #14.6, format(I6), required if (ISD(I).EQ.999) and
                             (GRNBLC(I) = 'NULL')
NBD(I)
      NBD(I)  : number of boundary loads for the ith component
                load used for thermal load only
```

```
Card #14.7.1, format(6E12.5), required if (ISD(I).EQ.999) and
                                         (GRNBLC(I) = 'NULL')
IDBDL(I,IBD),BDLNOM(I,IBD) for IBD=1,NBD(I)
      IDBDL(I,IBD)   : the ibd-th boundary load ID
                       for the ith component load
      BDLNOM(I,IBD) : the ibd-th boundary load nominal value

Card #14.7.2, format(I6), required if (ISD(I).EQ.999) and
                                     (GRNBLC(I) = 'NULL')
NBDDL(I,IBD)
      NBDDL(I,IBD) : number of dependent loads required in the
                     ibd-th boundary load influence model

Card #14.7.3, format(2E12.5), required if (ISD(I).EQ.999) and
                                         (GRNBLC(I) = 'NULL')
LCBDDL(I,IBD,IBDDL),MPBDDL(I,IBD,IBDDL),CINFBD(I,IBD,IBDDL)
for IBDDL=1,NBDDL(I,IBD)
      CLBDDL(I,IBD,IBDDL)  : load type of ibddl-th dependent load
                             for the ibd-th boundary load
                           = 0 system dependent load
                           = 1 component local load
      MPBDDL(I,IBD,IBDDL)  : dependency map of the ibd-th boundary
                             load to the dependent loads
      CINFBD(I,IBD,IBDDL)  : influence gain of the ibd-th boundary
                             load due to the corresponding
                             dependent load
Repeat card #14.7.3 input NBDDL(I,IBD) times
Repeat card #14.7.1-#14.7.3 input NBD(I) times

Card #14.8, format(I6), required if (ISD(I).EQ.999) and
                                    (GRNBLC(I) = 'NULL')
NODETM(I),NODEST(I),NODEBG(I)
      NODETM(I) : number of nodes for evaluation for the ith
                  component load
      NODEST(I) : do the component load calculation every other
                  NODEST(I) nodes
      NODEBG(I) : do the calculation starting from the NODEBG(I)
                  node


Card #15, format(6E12.5) required if GRNBLC <> NULL
CBLOAD(J), J=1,342
      CBLOAD : the scaling model coefficient set for component
               identified by ITBCOM
               temporary solution until the turbine blade
               geometry databases and the differential pressure
               load databases are built
```

```
Card #16, format(I6)
NGF
      NGF : number of geometry factor loads (component local
loads)
          = 0 if there is no geometry factor loads

Card #17, format(2I6,2E12.5), required if (NGF <> 0)
LGF(IGF),IGOGFL(IGF),GFLNOM(IGF),GFLCOV(IGF),IGF=1,NGF
      LGF(IGF)    : the igf-th geometry load ID
      IGOGFL(IGF): the distribution type
      GFLNOM(IGF): the nominal value
      GFLCOV(IGF): the coefficient of variation

Card #18.1, format(I6), repeat (card #18.1-#18.n) NRESP times
NMP(IR) for IR = 1 to NRESP
      NMP(IR) : number of mission history phase for ir-th
                dependent load

Card #18.2, format(A) required if (NMP(IR) <> 0)
TITLE
      TITLE : mission phase title

Card #18.3.1, format(I6,2E12.5), required if (NMP(IR) <> 0) and
                                 repeat (card #18.3.1-#18.3.n)
                                 NMP(IR) times
MP(IR,IMP),STIME(IR,IMP),ETIME(IR,IMP), for IMP = 1 to NMP(IR)
      MP(IR,IMP)      : mission phase type for the ir-th dependent
                        load & the imp-th mission phase
                        = 1 simple transient spike model
                        = 2 quasi-steady state
                        = 3 steady state
                        = 4 transient arrival model
                        = 5 transient arrival model with uniform
                            distribution for the number of random
                            spikes
      STIME(IR,IMP) : start time of the imp-th mission phase
      ETIME(IR,IMP) : end time of the imp-th mission phase

Card #18.3.2, format(I6,2E12.5) required if (MP(IR,IMP) = 1)
IDA(IR,IMP),AMP(IR,IMP),SDAMP(IR,IMP)
      IDA(IR,IMP)     : spike amplitude distribution type
      AMP(IR,IMP)     : mean spike amplitude
      SDAMP(IR,IMP) : standard deviation of the spike

Card #18.3.3, format(I6,2E12.5) required if (MP(IR,IMP) = 1)
IDT(IR,IMP),TIMEJ(IR,IMP),SDTJ(IR,IMP)
      IDT(IR,IMP)     : spike occurrence time distribution type
      TIMEJ(IR,IMP) : mean time of arrival
      SDTJ(IR,IMP)    : standard deviation of mean arrival time
```

Card #18.3.4, format(I6) required if (MP(IR,IMP) = 1)
NS

NS : number of simulation for the transient spike

Card #18.3.5, format(2I6), required if (MP(IR,IMP) >= 4)
NS,IDLAY

NS : number of simulation for transient spike arrival
IDLAY : fix delay time of the secondary spikes

Card #18.3.6, format(I6,2E12.5) required if (MP(IR,IMP) >= 4)
NFIX(IR,IMP),RAMDA(IR,IMP),WIDTH(IR,IMP)

NFIX(IR,IMP) : transient spike arrival type
< 0 for subsequent spikes to arrive at an IDLAY WIDTH later
= 0 for spikes to arrive at a mean time TIMEJ(IR<IMP) input next
> 0
RAMDA(IR,IMP) : transient spike mean arrival rate
WIDTH(IR,IMP) : transient spike width parameter

Card #18.3.7, format(I6,2E12.5), required if (MP(IR,IMP) >= 4)
IDA, AMP(IR,IMP), SDAMP(IR,IMP)

IDA(IR,IMP) : distribution type for the spike amplitude
AMP(IR,IMP) : spike amplitude mean value
SDAMP(IR,IMP): spike amplitude standard deviation

Card #18.3.8, format(I6,2E12.5), required if (MP(IR,IMP) >= 4)
IDT(IR,IMP),TIMEJ(IR,IMP),SDTJ(IR,IMP)

IDT(IR,IMP) : spike occurrence time distribution type
TIMEJ(IR,IMP): mean occurrence time
SDTJ(IR,IMP) : standard deviation of the occurrence time

REPORT DOCUMENTATION PAGE

Form Approved
OMB No. 0704-0188

1. AGENCY USE ONLY (*Leave blank*)

2. REPORT DATE
December 1991

3. REPORT TYPE AND DATES COVERED
Final Contractor Report

4. TITLE AND SUBTITLE
Composite Load Spectra for Select Space Propulsion Structural Components
(Opton I—Final Report)

5. FUNDING NUMBERS
WU-555-13-00
C-NAS3-24382

6. AUTHOR(S)
James F. Newell and Hing W. Ho

7. PERFORMING ORGANIZATION NAME(S) AND ADDRESS(ES)
Rockwell International
Rocketdyne Division
6633 Canoga Avenue
Canoga Park, California 91304

8. PERFORMING ORGANIZATION REPORT NUMBER
None

9. SPONSORING/MONITORING AGENCY NAMES(S) AND ADDRESS(ES)
National Aeronautics and Space Administration
Lewis Research Center
Cleveland, Ohio 44135-3191

10. SPONSORING/MONITORING AGENCY REPORT NUMBER
NASA CR-189078
RI/RD 91-219

11. SUPPLEMENTARY NOTES
Project Manager, C.C. Chamis, Structures Division, NASA Lewis Research Center, (216) 433-3252.

12a. DISTRIBUTION/AVAILABILITY STATEMENT
Unclassified - Unlimited
Subject Category 39

12b. DISTRIBUTION CODE

13. ABSTRACT ***(Maximum 200 words)***
This report summarizes the development for (1) correlation fields, (2) applications to Lox post, (3) models for pressure fluctuations and vibration loads fluctuations, (4) additions to expert system, and (5) scaling criteria. Implementation to computer code is also described. Demonstration sample cases are included with additional applications to engine duct and pipe bend.

14. SUBJECT TERMS
Correlation fields; Pressure fluctuations; Vibration loads; Expert system; Coupled loads; Engine duct; Pipe bend; Scaling criteria; Computer code; Sample cases

15. NUMBER OF PAGES

16. PRICE CODE

17. SECURITY CLASSIFICATION OF REPORT	18. SECURITY CLASSIFICATION OF THIS PAGE	19. SECURITY CLASSIFICATION OF ABSTRACT	20. LIMITATION OF ABSTRACT
Unclassified	Unclassified	Unclassified	

NSN 7540-01-280-5500

Standard Form 298 (Rev. 2-89)
Prescribed by ANSI Std. Z39-18
298-102